

RAPPORT

Jürgen König, Lars Walleij

**One-Dimensional Charring of Timber
Exposed to Standard and Parametric Fires
in Initially Unprotected and
Postprotection Situations**

Träteknik

Jürgen König, Lars Walleij

ONE-DIMENSIONAL CHARRING OF TIMBER EXPOSED TO
STANDARD AND PARAMETRIC FIRES IN INITIALLY
UNPROTECTED AND POSTPROTECTION SITUATIONS

Trätekt, Rapport I 9908029

ISSN 1102 – 1071

ISRN TRÄTEK – R – – 99/029 – – SE

Nyckelord

charring
fire
modelling
protection
tests
timber
wood

Stockholm augusti 1999

Rapporter från Trätec — Institutet för träteknisk forskning — är kompletta sammanställningar av forskningsresultat eller översikter, utvecklingar och studier. Publicerade rapporter betecknas med I eller P och numreras tillsammans med alla utgåvor från Trätec i löpande följd.

Citat tillåtes om källan anges.

Reports issued by the Swedish Institute for Wood Technology Research comprise complete accounts for research results, or summaries, surveys and studies. Published reports bear the designation I or P and are numbered in consecutive order together with all the other publications from the Institute.

Extracts from the text may be reproduced provided the source is acknowledged.

Trätec — Institutet för träteknisk forskning — betjänar de fem industrigrenarna sågverk, trämanufaktur (snickeri-, trähus-, möbel- och övrig träförädlingsindustri), träfiberskivor, spånskivor och plywood. Ett avtal om forskning och utveckling mellan industrin och Nutek utgör grunden för verksamheten som utförs med egna, samverkande och externa resurser. Trätec har forskningsenheter i Stockholm, Jönköping och Skellefteå.

The Swedish Institute for Wood Technology Research serves the five branches of the industry: sawmills, manufacturing (joinery, wooden houses, furniture and other woodworking plants), fibre board, particle board and plywood. A research and development agreement between the industry and the Swedish National Board for Industrial and Technical Development forms the basis for the Institute's activities. The Institute utilises its own resources as well as those of its collaborators and other outside bodies. Our research units are located in Stockholm, Jönköping and Skellefteå.

Contents

Preface.....	2
Summary.....	3
Sammanfattning - Swedish summary.....	4
Summary.....	3
1 Introduction.....	5
2 Fire tests.....	8
2.1 General.....	8
2.2 Testing equipment, specimens and material.....	8
2.3 Series A: Standard fire exposure of initially unprotected timber.....	12
2.4 Series B: Standard fire exposure of initially protected timber.....	16
2.5 Series C: Parametric fire exposure of initially unprotected timber.....	22
3 Modelling.....	29
3.1 General.....	29
3.2 Calibration of material properties.....	29
3.2.1 Standard fire exposure.....	29
3.2.2 Parametric fire exposure.....	36
3.3 Charring depth at parametric fire exposure according to Eurocode 5.....	40
4 Conclusions.....	43
4.1 Tests.....	43
4.2 Model.....	43
5 References.....	45

Preface

The investigations reported here, carried out by Trätec - Swedish Institute for Wood Technology Research, were part of the Nordic research project "Fire safe wooden buildings" within the Nordic Wood Programme. The project has been funded by Swedish, Norwegian and Finnish timber and building materials industry, national funds and the Nordic Industrial Fund which is kindly acknowledged. The work reported here has been funded by

Träforsk – The Association for Swedish Wood Products Research

Brandforsk – The Swedish Fire Research Board

NUTEK – Swedish National Board for Industrial and Technical Development.

Summary

The research that is reported here deals with charring of timber members of spruce exposed to fire with thermal conditions of one-dimensional heat transfer as in semi-infinite slabs. The tests were conducted using a small-scale furnace. The members were exposed to ISO 834 standard fire or parametric fires representing natural fire scenarios of different degrees of severity. At standard fire exposure, the charring rate during the post-protection phase of initially protected members was compared with the charring rate of initially unprotected members.

In the first series consisting of four tests the member was unprotected right from the start of the standard fire exposure, whereas, in the second series, the member was protected during the initial phase until a temperature of 300°C was reached at the interface between the protection and the wood member, indicating the onset of charring of the member. The second series consisted of five tests where the members were protected by particleboard or gypsum plasterboard during the initial period of length between 24 and 70 minutes. Where the protection was made of gypsum plasterboard, the sheets were immediately released at the time of onset of charring. Whereas the charring depth varies almost linearly in initially unprotected members, during the post-protection phase the relationship between time and charring depth is pronounced non-linear, with charring rates generally greater than in the case of initially unprotected members.

The six tests of the third series were performed using parametric fire curves. The results of charring rates confirm the expressions for charring depth given in the Fire Part of Eurocode 5, based on the work by Hadvig and later by Bolonius Olesen.

The results of the tests with standard fire exposure were used in order to determine the conductivity and specific heat of wood by calibrating them to the test results using the computer program TEMPCALC for calculation of heat transfer. The calibration was necessary, since, even though thermal properties were physically correct they often would give incorrect results due to the model not taking into account mass transfer and changes in the structure e.g. the cracking of charcoal. It was found that the heat of reaction during pyrolysis could be neglected. The data obtained were compared with the data from other sources, comprising considerable scatter. One of the conclusions is that thermal properties taken from different sources may give unduly conservative or unsafe results if they are used in the design without calibrating them to test results.

Calculations using the thermal properties that were calibrated to test results with standard fire exposure overpredict the charring rate when the temperature rise is greater than at standard fire exposure, i.e. when the opening factor is greater than $0,04 \text{ m}^{1/2}$, whereas they underpredict the charring rate when the gas temperature is decreasing during the decay phase. Therefore, for parametric fire curves, charring of timber should be studied further.

SAMMANFATTNING

I denna rapport behandlas inbränning i trä (gran) där de termiska förhållandena motsvarar dem som existerar vid endimensionell värmetransport in i en halvrymd av trä eller en mycket tjock träplatta. Försöken genomfördes i en modellugn. Träet exponerades för brandpåverkan motsvarande standardbrandkurvan enligt ISO 834 eller parametriska brandkurvor som representerar olika naturliga brandförlopp. Avseende standardbrandpåverkan jämfördes inbränningen hos trä som varit oskyddat från början med inbränningen hos trä som varit skyddat under en viss period i början av brandexponeringen.

I den första försöksserien bestående av fyra försök var träet oskyddat från början medan det i den andra serien var skyddat under den initiala fasen tills temperaturen på träets yta nådde 300°C då trä börjar förkolna. Den andra serien bestod av fem försök där träet skyddades av spån- eller gipsskivor under den initiala perioden som varade mellan 24 och 70 minuter. När gipsskivor användes släpptes de så fort inbränningen i träet börjat. Hos från början oskyddat trä ökar inbränningsdjupet tämligen linjärt med tiden medan sambandet är påtagligt olinjär i efterskyddsfasen där inbränningshastigheten generellt är större än hos från början oskyddat trä.

De sex försöken i den tredje serien genomfördes med parametriska brandkurvor. Resultaten bekräftar uttrycken för inbränningsdjup enligt branddelen av Eurokod 5 som är baserade på Hadvigs och senare Bolonius Olesens arbeten.

Resultaten från försöken med standardbrandbelastning användes för att bestämma värmeledningen och den specifika värmekapaciteten hos trä genom att kalibrera dem med avseende på den uppmätta inbränningen med hjälp av dataprogrammet TEMPCALC för beräkning av värmetransport. Även om man använde fysikaliskt korrekta termiska egenskaper vid beräkningarna så skulle resultaten ofta bli inkorrekta eftersom beräkningsmodellen varken beaktar masstransport eller materialets strukturförändringar, t. ex. kolskiktets krackelering. Det kunde visas att reaktionsvärmen vid pyrolysen är försumbar. De erhållna termiska egenskaperna jämfördes med data från andra källor som uppvisar betydande spridning. En av slutsatserna är att användningen av termiska egenskaper från litteraturen kan leda till onödigt konservativa eller osäkra resultat om de används vid brandtekniska beräkningar utan kalibrering med avseende på försöksresultat.

Beräkningar med termiska egenskaper som kalibrerats med avseende på standardbrand överskattar den initiala inbränningshastigheten när temperaturstegringen är större än vid standardbrand (d. v. s. när öppningsfaktorn är större än $0,04 \text{ m}^{1/2}$) medan de underskattar inbränningshastigheten när gastemperaturen avtar under avsvlningsfasen. Därför bör träets inbränning vid naturligt brandförlopp studeras ytterligare.

1 Introduction

In most design codes for structural fire design, charring rates are given for various wood species. These values are design values that can be used under certain conditions. During the last decades, the charring rates given by various design codes have varied considerably, e.g. for softwoods with values between 0,6 and 1,1 mm/minute. Often these design charring rates are or were notional values since they may or could include the effect of strength and stiffness degradation due to elevated temperatures or the effect of increased charring at cross section arrises and fissures. The charring rate is or was not regarded solely as a material property. In the Fire Part of Eurocode 5¹, an attempt was made to consider the charring rate as a material property, however not rigorously. A notional charring rate was introduced in order to simplify the design, i.e. it should be possible to assume that the residual cross section was a rectangle or built up of several rectangles. Effects of degradation of strength and stiffness parameters should be regarded separately.

Due to the lack of a standard for determining charring rates, in Eurocode 5 no proper definition of the term charring rate was given, nor how appropriate design charring rates should be derived from the results of fire tests. It should be one of the tasks during the redrafting of the Fire Part of Eurocode 5 to give this basic information. In a previous paper² it was proposed to define a basic charring rate as the charring rate at one-dimensional heat transfer under the thermal conditions of a semi-infinite slab. All other charring rates, e.g. notional charring rates in order to include the effects of arris roundings, charring rates of smaller cross sections and charring rates of protected members should be related to the basic charring rate. One of the objectives of the investigation reported here was to provide information to be considered during the redrafting.

During several years in the past comprehensive research was conducted in order to study the fire behaviour of timber framed wall and floor assemblies^{3,4}. Charring rates were determined for timber frame members, however due to the influence of the shape of the cross section, the charring rates were greater than observed from tests with large cross sections, e.g. glued laminated beams. In order to make available the findings of the above mentioned research results for designers, a design model was developed⁵. In this model the charring rates are given in relation to the basic charring rate at one-dimensional charring of timber assuming the thermal conditions of a semi-infinite slab. Therefore, it was necessary to perform additional fire tests with one-dimensional heat transfer. In order to perform calculations of heat transfer in timber frame members it was felt appropriate to make a calibration of the thermal properties of timber using the well-defined thermal conditions as they can be obtained at one-dimensional heat transfer. The results of this calibration are shown in chapter 3 of this report.

Previously⁴, with respect to charring, in general the following protection and charring phases were identified, see:

- Charring phase I of initially unprotected wood, see Figure 1.1
- Protection phase before failure of boards, see Figure 1.2
 - Pre-charring phase (complete protection)
 - Charring phase II (incomplete protection)
- Post-protection phase after failure of boards: charring phase III, see Figure 1.2 and Figure 2.1.

For simplicity, linear relationships were assumed between the charring depth and time.

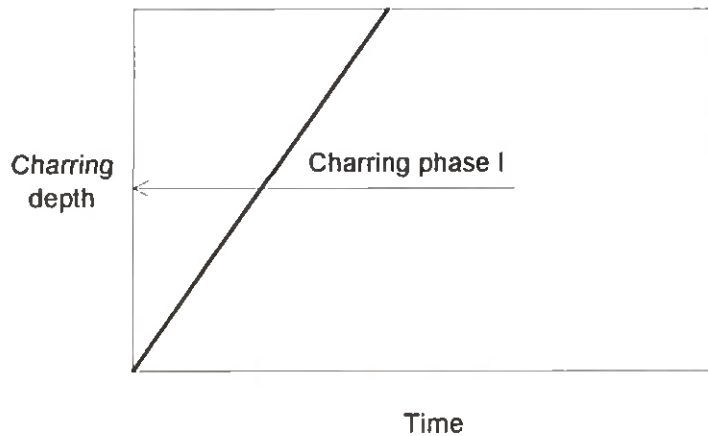


Figure 1.1: Charring phase I - initially unprotected wood

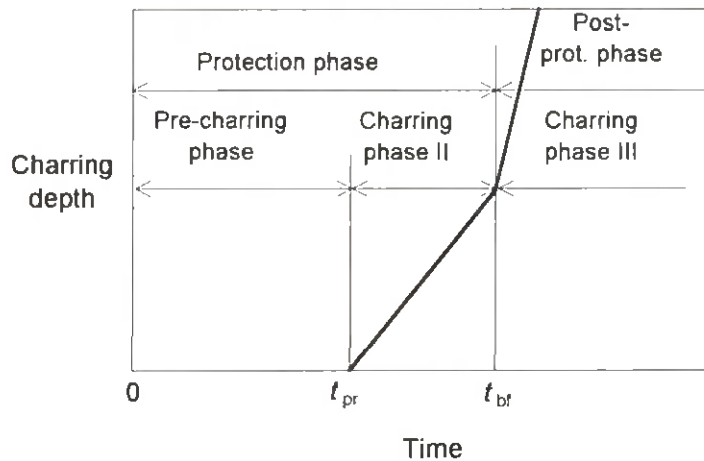


Figure 1.2: Charring phases of protected wood in general

The charring rates during charring phase II and III are different from the charring rate of initially unprotected members (phase I), depending on the temperature in the fire compartment or furnace and, in the case of non-combustible claddings, also on the insulation provided by the cladding. Therefore, one of the objectives of this investigation was to determine the charring rate of timber during the post-protection phase.

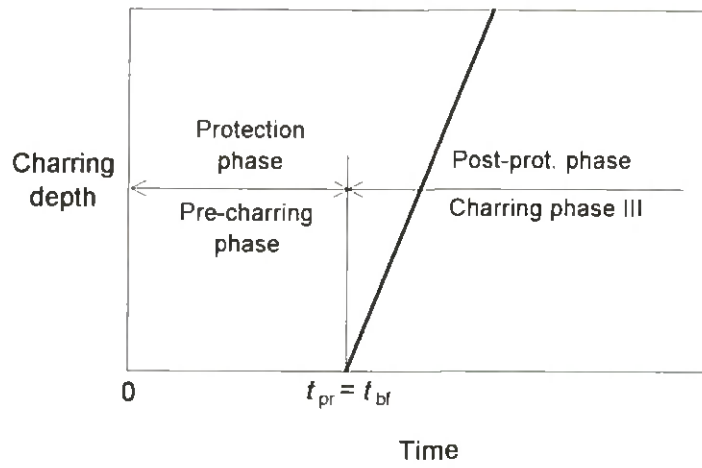


Figure 1.3: Charring phases of wood protected by wood-based boards

2 Fire tests

2.1 General

The fire tests reported here were subdivided into three series:

- Series A: Standard fire exposure of initially unprotected timber
- Series B: Standard fire exposure of initially protected timber
- Series C: Parametric fire exposure of initially unprotected timber

The fire tests were performed using the standard fire curve according to ISO 834 (in the following also called SFE) and two parametric fire curves⁶, see Figure 2.1. The parametric fire curves are defined by the fire load density in MJ/m² related to the total area of the enclosure of the fire compartment and the opening factor in m^{1/2}.

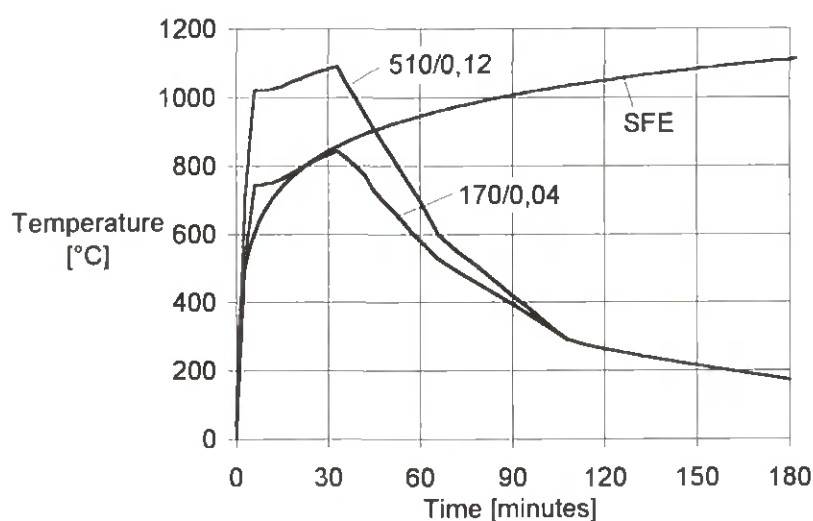


Figure 2.1: Fire curves used in the fire tests

2.2 Testing equipment, specimens and material

A small gas-fired furnace with interior cladding of mineral wool was used in the fire tests. Its interior length was 1 m, and its width and depth were 0,6 m. See Figure 2.2. The furnace was covered by the specimen itself, or by the specimen and additional sheets of calcium silicate or gypsum plasterboard. The furnace temperature was measured by means of a plate thermometer located in the middle of the furnace 100 mm below the lower side of the test specimen. In order to allow visual observation of the specimen during the fire test, an opening was located in the middle of the wide side 300 mm below the specimen.

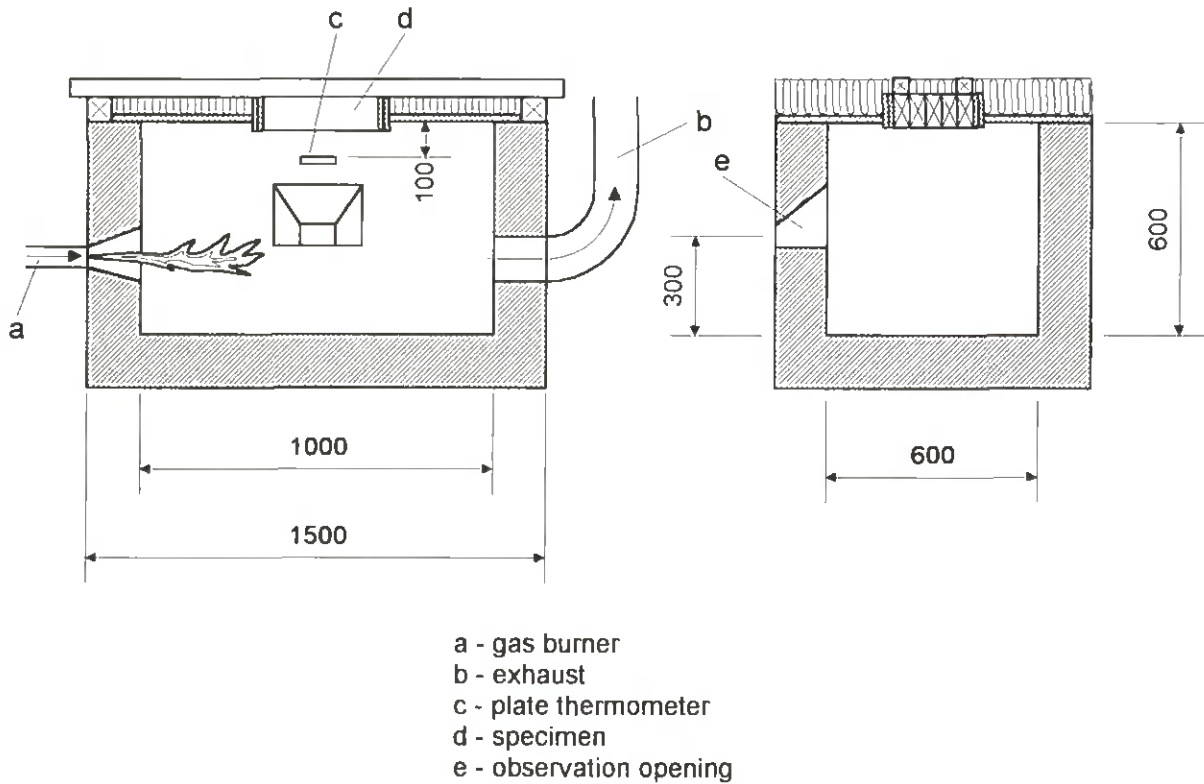


Figure 2.2: Small-scale furnace and arrangement of specimen

Each specimen was built up of the timber member itself and additional materials in order to provide one-dimensional heat transfer through the timber, and, in series A and B, to form a cover of the furnace, see Figure 2.3. The timber member was built up of 5 pieces of timber with dimensions 45 mm × 95 mm connected by gluing such that the resultant cross section was 225 mm × 95 mm. The members were of spruce with a dry density of 420-430 kg/m³. Before testing the specimens were conditioned at 20°C and 65 % RH.

In **series A** the length of the member was 1000 mm, see Figure 2.3. The narrow sides of the member were protected by two layers of 15,4 mm thick sheets of gypsum plasterboard type F screwed onto it and the remaining space of the specimen filled with rock fibre insulation of density 28 kg/m². The top of the specimen was made of one layer of gypsum plasterboard type F, while the lower side was covered by two layers leaving the middle part of the member unprotected.

All thermocouples for registration of the temperature in the timber member were of chromel-alumel, type K. For their location see Figure 2.4.

The specimens of **series B** were identical to those of series A, except that the middle part of the member was protected by one or two pieces of board for initial protection of the member. These boards are specified in Table 2.1. Where pieces of particleboard were used, they were screwed to the member with four screws near the corners, whereas pieces of gypsum plasterboard were fixed to the member such that they could be released during the test.

Table 2.1: Initial protection of members in series B

B1	16 mm particleboard
B2	16 mm particleboard
B3	2 × 16 mm particleboard
B4	2 × 15,4 mm gypsum plasterboard GF
B5	2 × 15,4 mm gypsum plasterboard GF

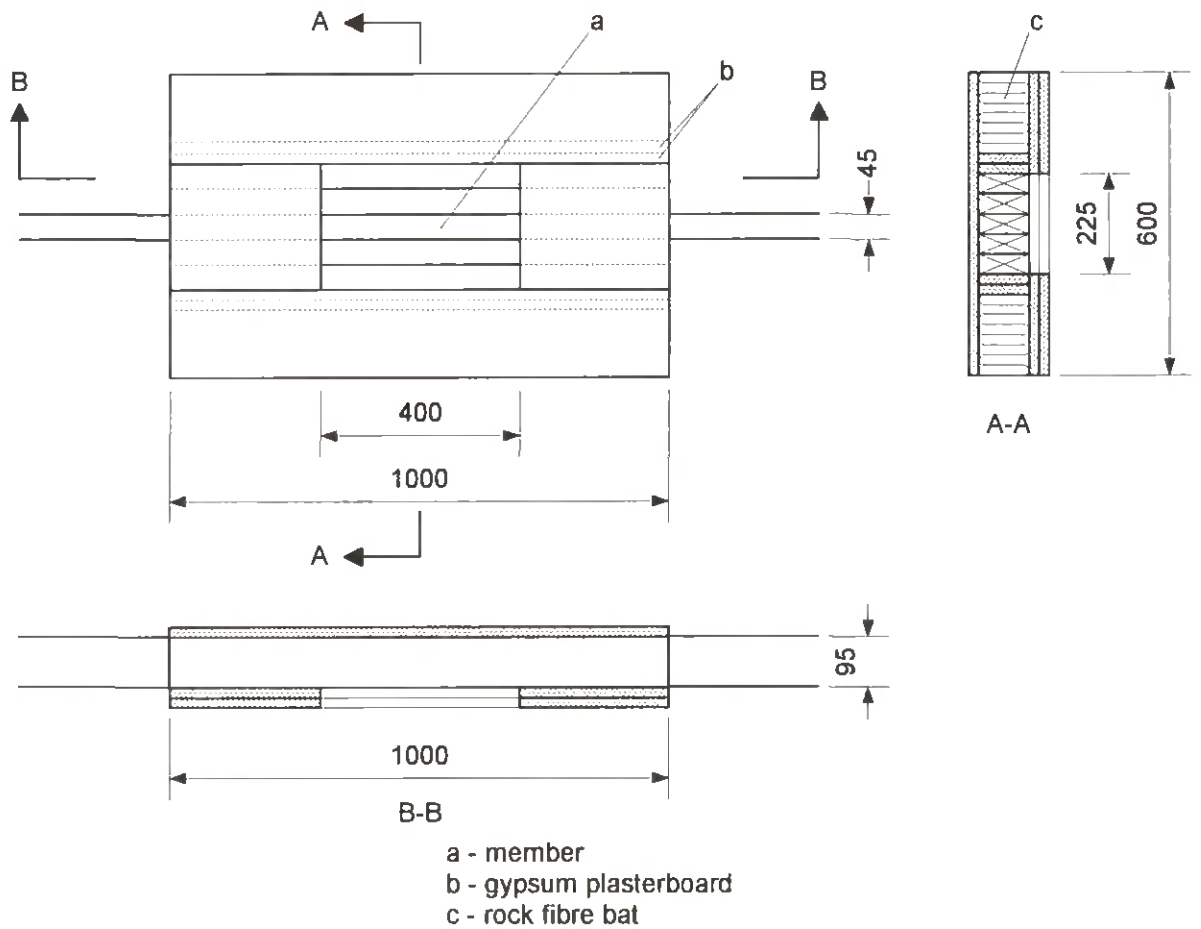


Figure 2.3: Test specimens of series A

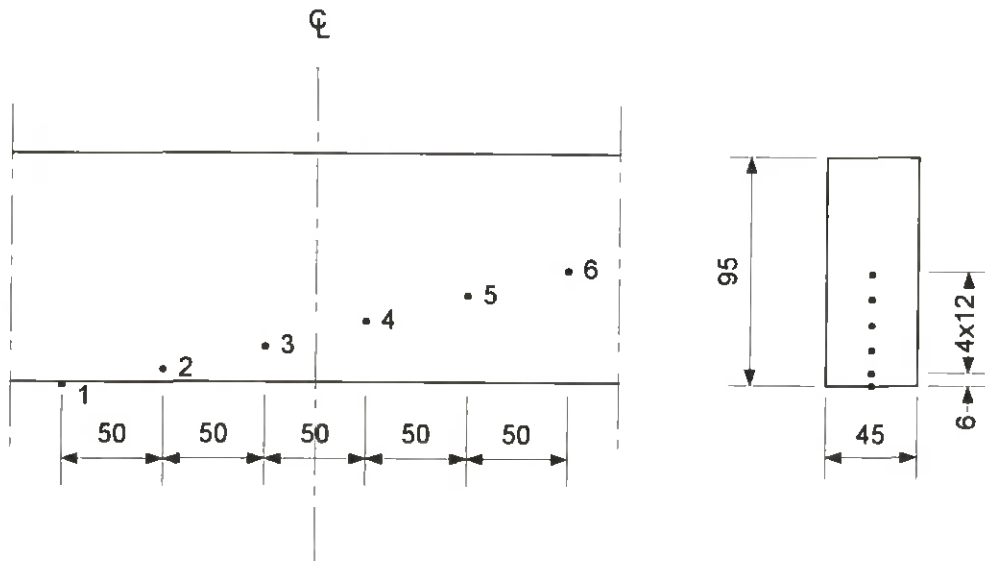


Figure 2.4: Location of thermocouples in the middle piece of the member in test series A and B

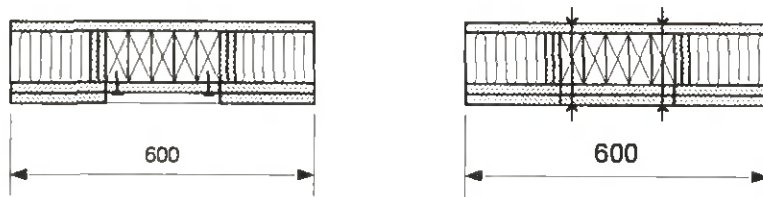


Figure 2.5: Fixing of initial protection of members of series B (c.f. section A-A in Figure 2.3)

In **series C** the length of the member was 325 mm, see Figure 2.6. The four narrow sides of the member were protected by two layers of gypsum plasterboard. The member was fixed to two wooden sticks of dimension 45 mm × 45 mm that were supported by the furnace walls, see Figure 2.2. The remaining surface of the furnace was covered by sheets of calcium silicate or gypsum plasterboard and a 95 mm thick layer of rock fibre bats. The location of thermocouples was similar to series A and B with a spacing of 25 mm, see Figure 2.7.

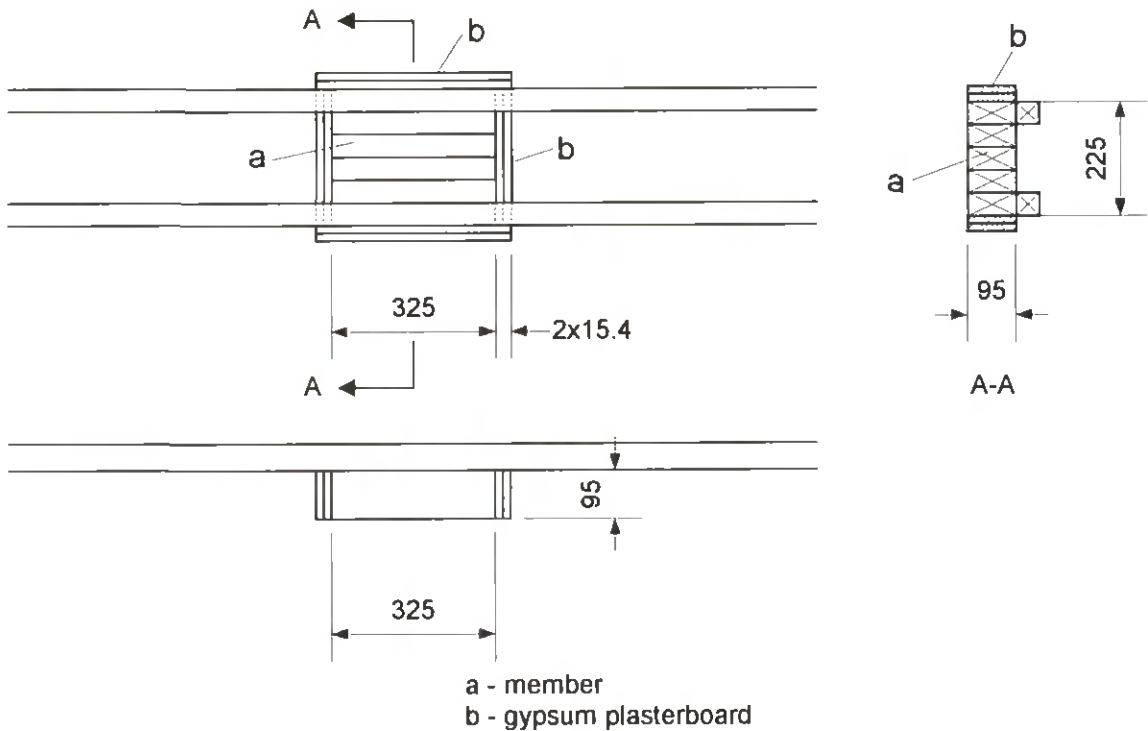


Figure 2.6: Test specimens of series C

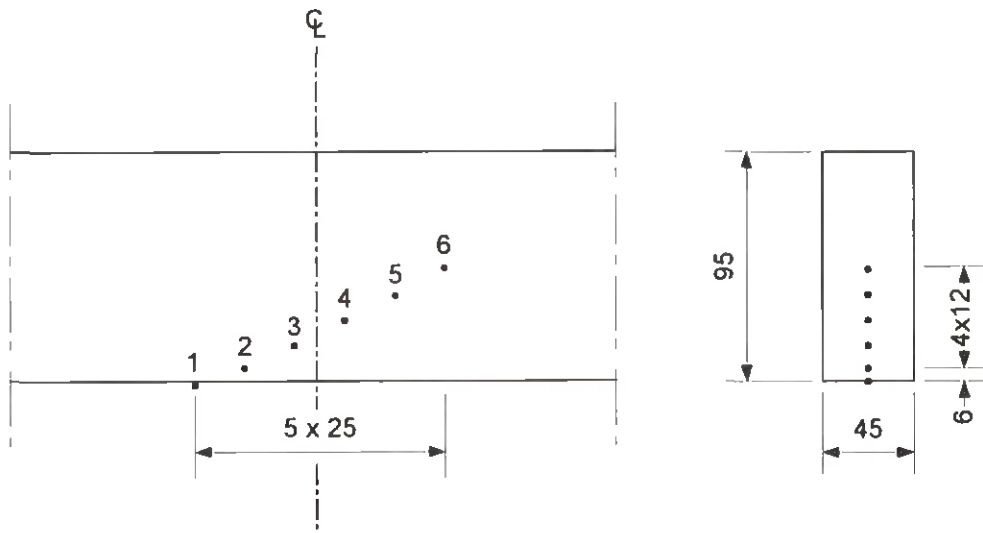


Figure 2.7: Location of thermocouples in the middle piece of the member in test series C

2.3 Series A: Standard fire exposure of initially unprotected timber

The fire tests were discontinued when the charring depth exceeded 54 mm, i.e. when the temperature measured at a distance of 54 mm from the original surface of the member (gauge point 6) exceeded 300°C.

The recorded temperature-time relationships are shown in Figure 2.8 and 2.9.

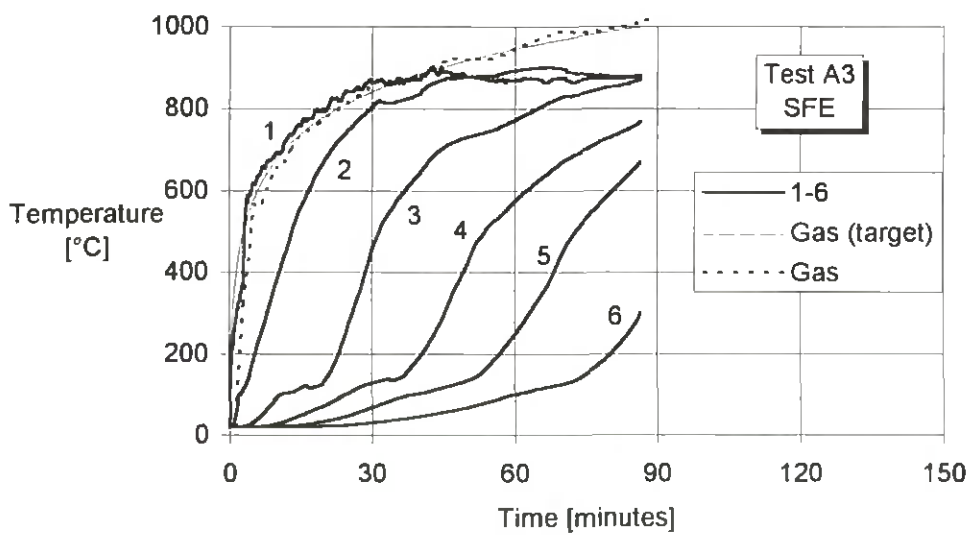
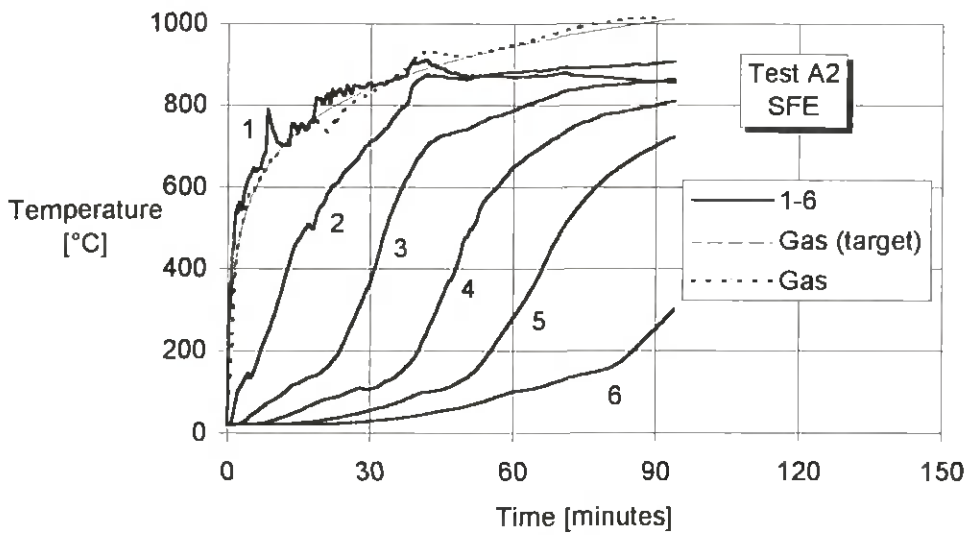
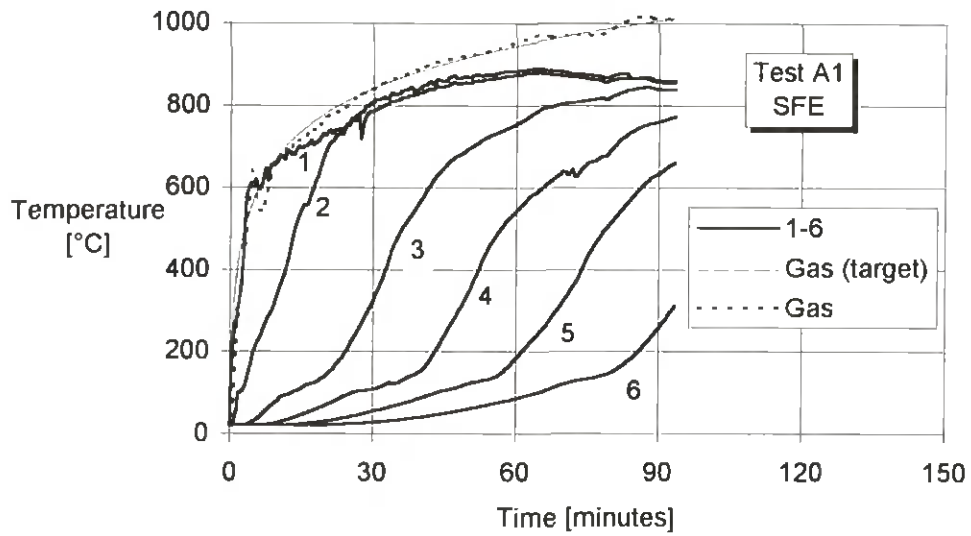


Figure 2.8: Temperature-time relationships of tests A1-A3 (initially unprotected member)

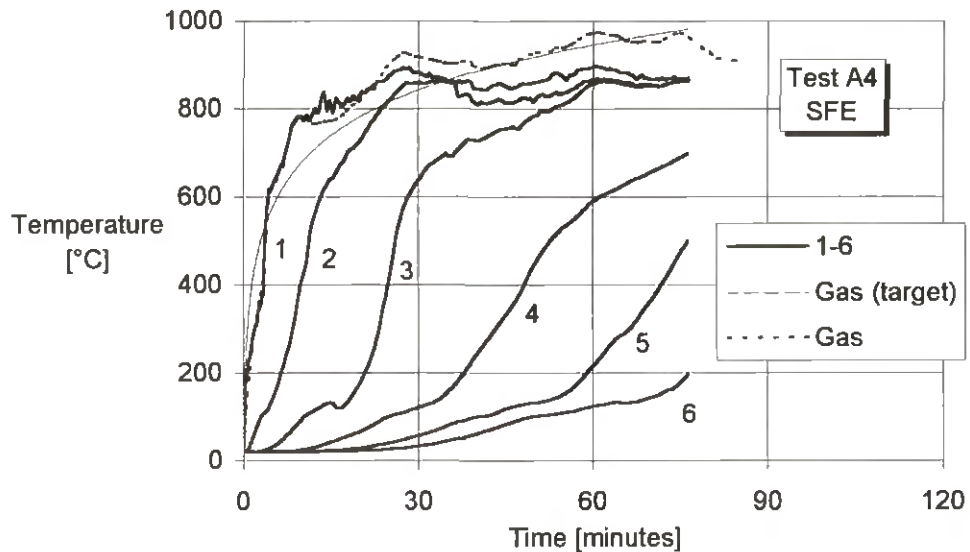


Figure 2.9: Temperature-time relationships of test A4 (initially unprotected member)

Temperature profiles are shown in Figure 2.10 for temperatures up to 300°C, i.e. the temperature at the char line. We can see that a depth of about 35 mm is already affected by the fire after about 10 minutes, and that this depth is fairly constant thereafter.

The increase of the charring depth, defined as the 300-degree isotherm, is shown in Figure 2.4. In test A4 the gas temperature deviated considerably from the target fire curve, see Figure 2.9, giving rise to a slightly greater charring rate than in the other tests. The temperature measured at gauge point 1 indicates that charring started after 1,5 to 2 minutes. This could also be observed by viewing the test specimen through the observation opening in the furnace wall. The relationships between the charring depth and time are fairly constant, however with a slightly decreasing slope after some time, depending on the thermal insulation by the increasing char layer.

Using the recorded charring depths of tests A1 to A3, two regression curves were determined, one of them with an intercept equal to zero, see Figure 2.13. The corresponding mean charring rates, i.e. the secant values determined with the assumption that charring starts at time zero, are shown in Figure 2.14. The secant value of the charring rate varies linearly between 0,7 mm/minute after 20 minutes and 0,6 mm/minute after 90 minutes. The value given in the Fire Part of Eurocode 5¹ is 0,64 mm/minute and corresponds to a time of fire exposure of 60 minutes.

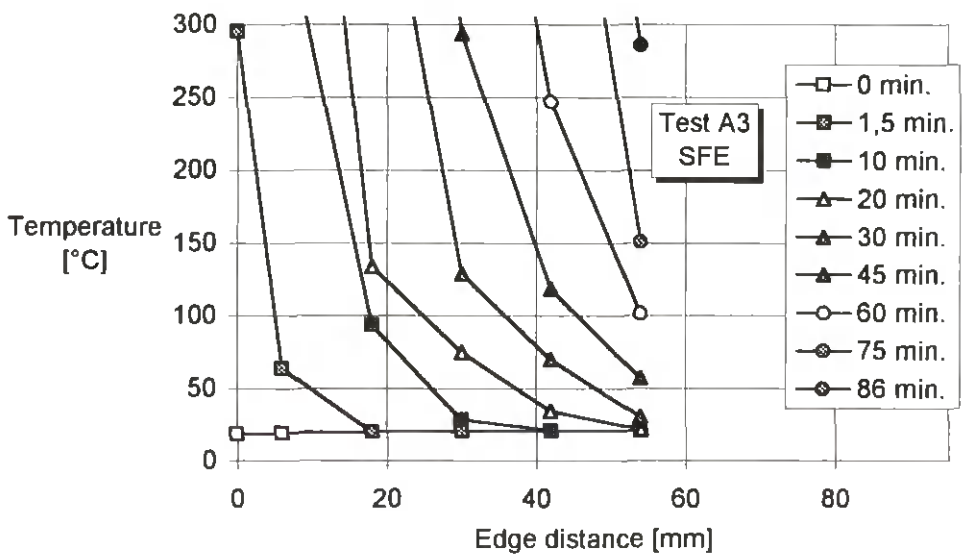
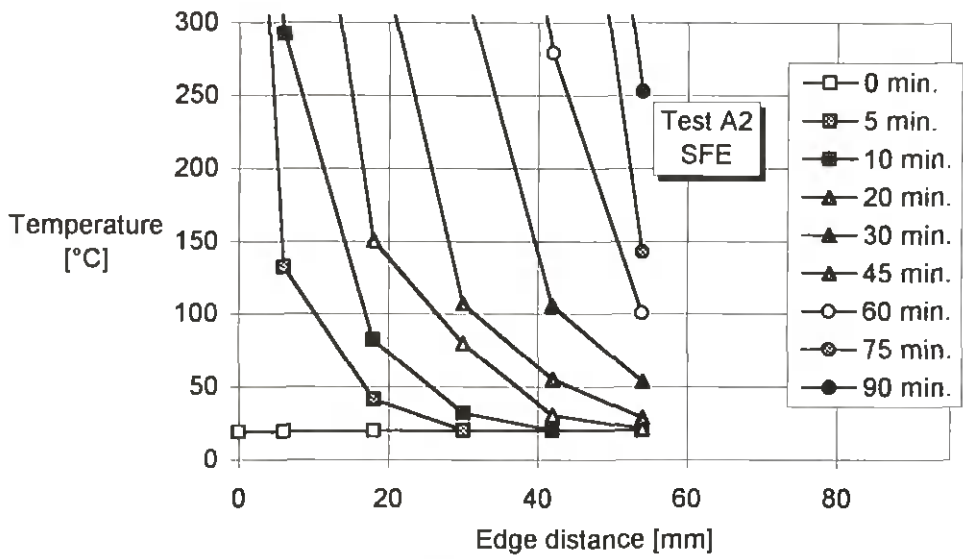
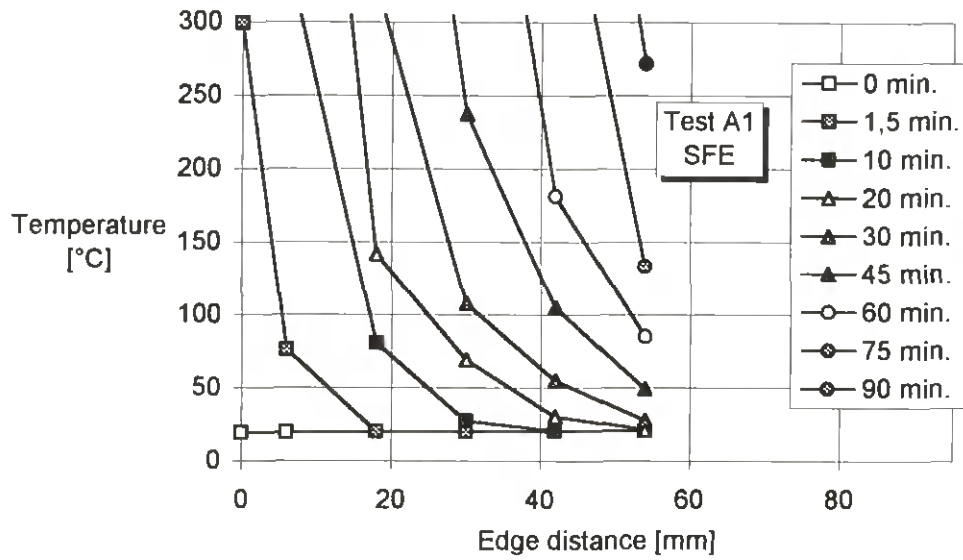


Figure 2.10: Temperature profiles in members of series A (initially unprotected member)

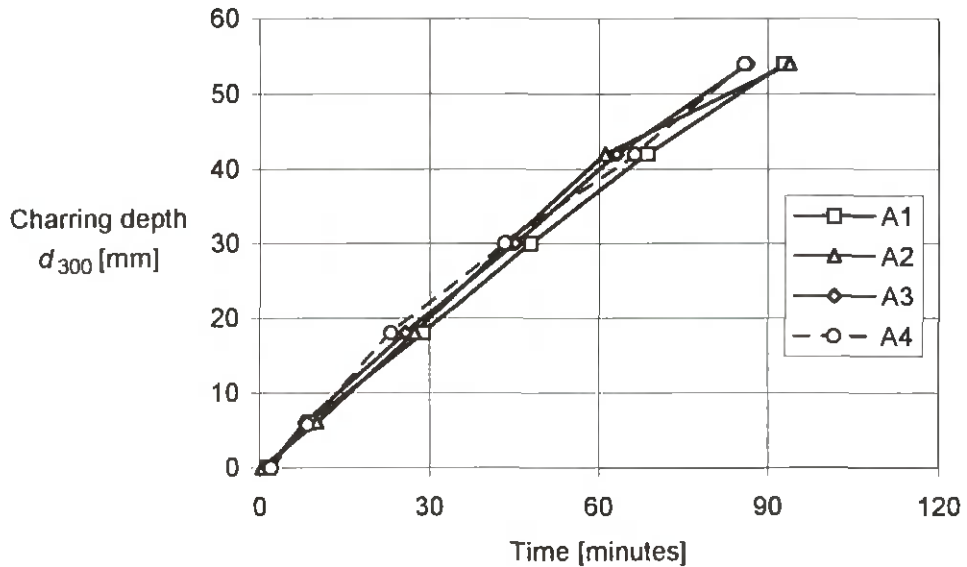


Figure 2.11: Charring depth versus time of series A

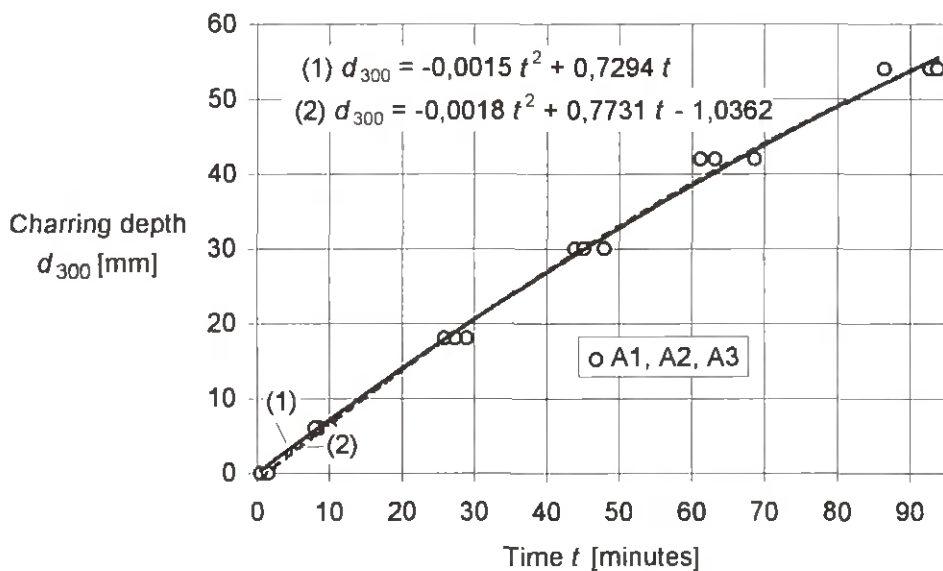


Figure 2.13: Regression curves for charring depth versus time

2.4 Series B: Standard fire exposure of initially protected timber

During these tests the post-protection phase started at the time of onset of charring. At that time in tests B1-B3 the initial protection of particleboard was charred and the remaining parts of the charcoal fell off the member. In order to achieve post-protection conditions immediately after the onset of charring, in tests B4 and B5 the pieces of gypsum plasterboard providing the initial protection of the member were released at the time of onset of charring, i.e. when the temperature at gauge point 1 exceeded 300°C. The tests were discontinued when the temperature at gauge point 6 reached 300°C.

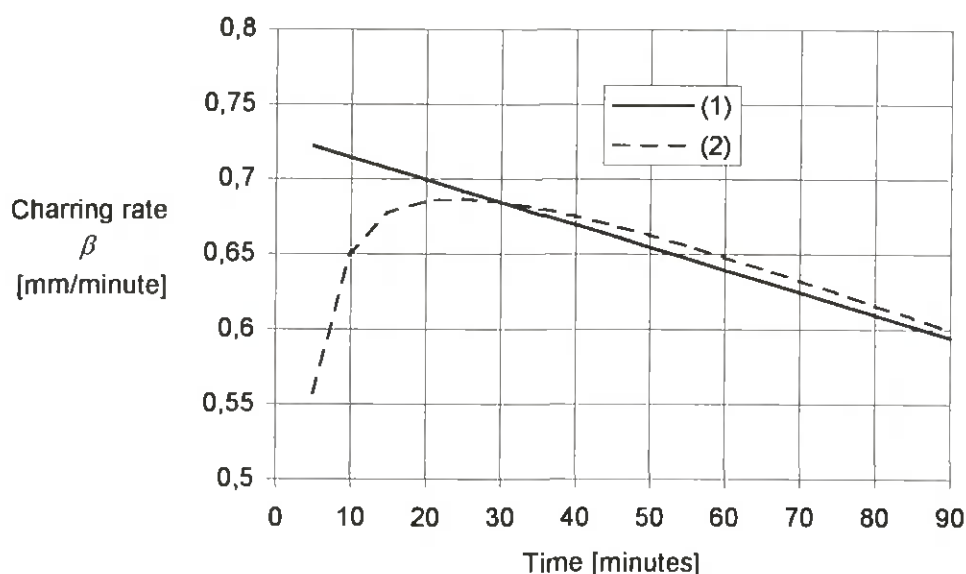


Figure 2.14: Mean charring rates versus time for regression curves shown in Figure 2.13

The recorded time-temperature relationships are shown in Figure 2.14 and 2.15. In test B4, unfortunately, still during the protection phase, the tests was interrupted after 31 minutes due to a breakdown of the furnace. At that time the temperature was 800°C. A few minutes later the furnace was restarted and the standard fire curve was followed from a somewhat lower temperature. The data obtained onward from the time when the temperature reached 800°C again were linked together with the data from the first period of the test. Therefore, the value of t_{pr} (see the definition given in Figure 1.2) from test B4 is not relevant for a protection of two layers of gypsum plasterboard type F (GF). For continuous standard fire exposure, the correct value of t_{pr} is obtained from test B5.

Temperature profiles in the member are shown in Figure 2.16 and Figure 2.17. At the time of onset of charring all members exhibit similar temperature profiles, independent of the material of the protective boards.

As before, the propagation of the char-line is shown as the position of the 300-degree isotherm, see Figure 2.18. For comparison, the figure shows also the curves of series A from Figure 2.11. Contrary to the results of series A, the relationship between the charring depth and time is significantly non-linear. Especially the initial slope of the charring-depth time curves is considerably greater than in series A, since the unprotected surface of the member is exposed to higher temperatures. When the thickness of the char layer is about 10-15 mm the charring rate decreases again. We can see that the initial and final slopes of the curves are dependent on the time of charring, or indirectly, on the temperature in the furnace.

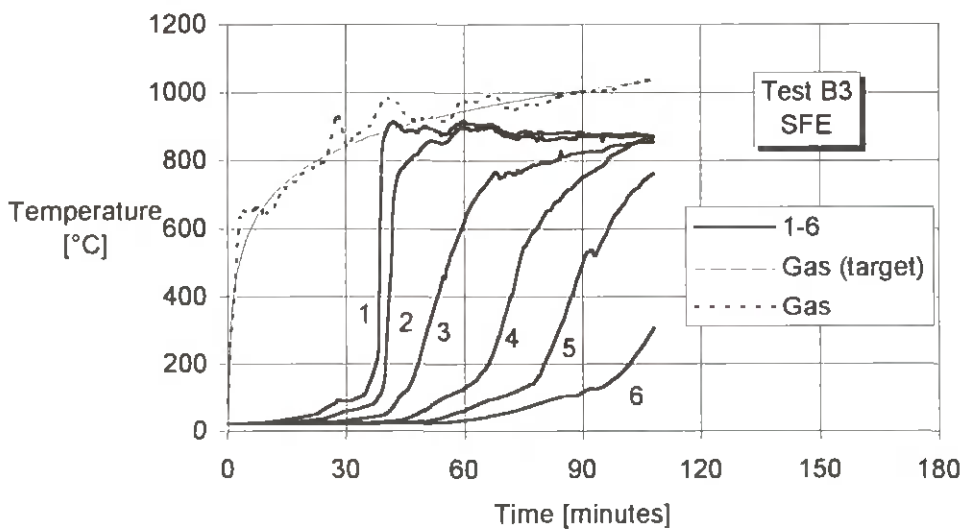
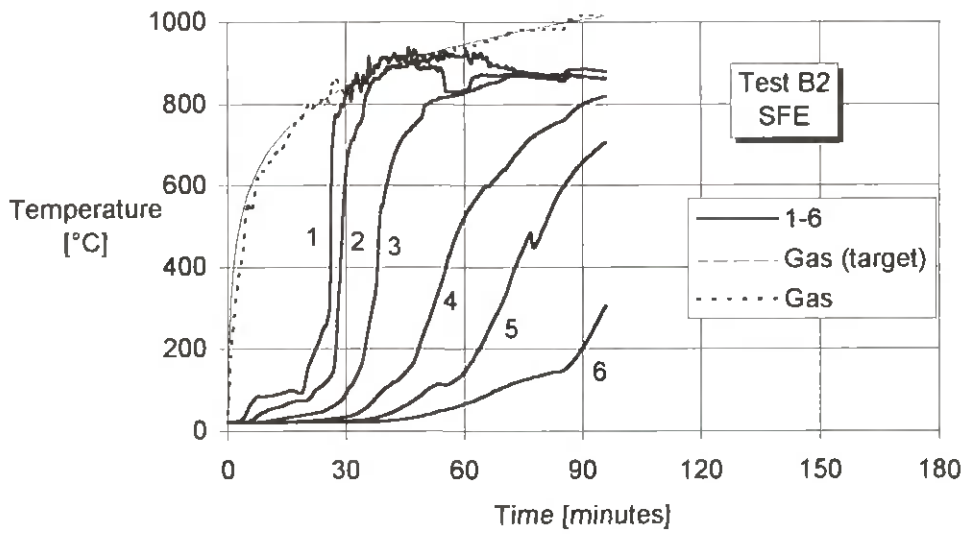
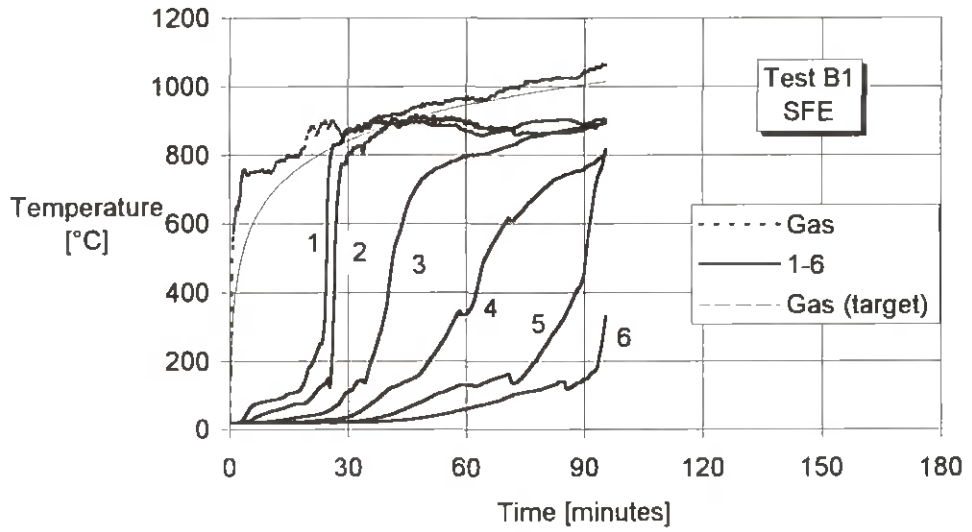


Figure 2.14: Temperature-time relationships of tests B1-B3 (initially protected member)

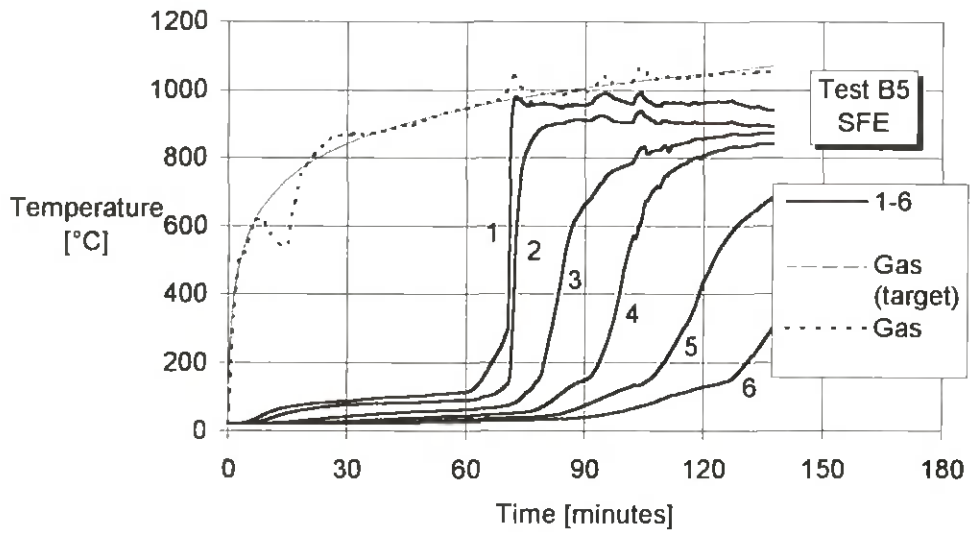
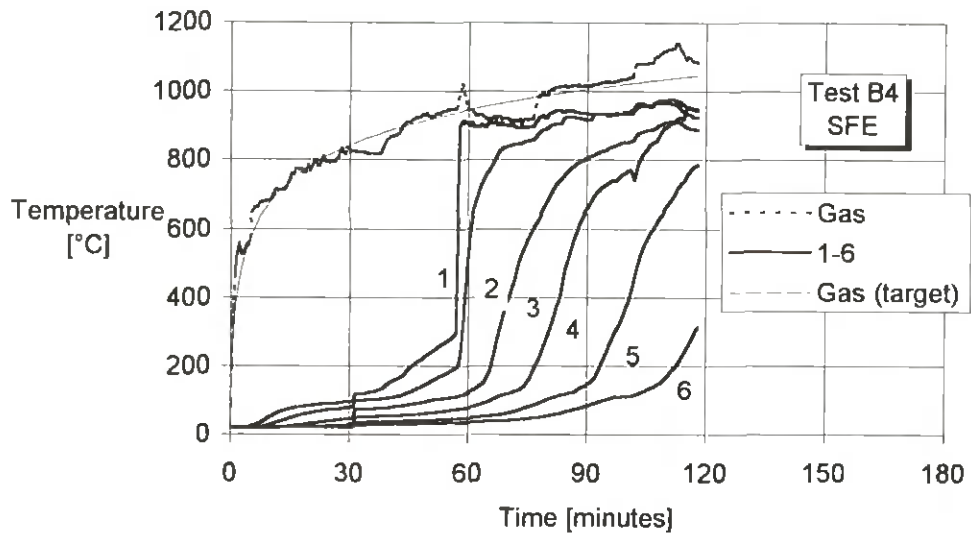


Figure 2.15: Temperature-time relationships of tests B4 and B5 (initially protected member)

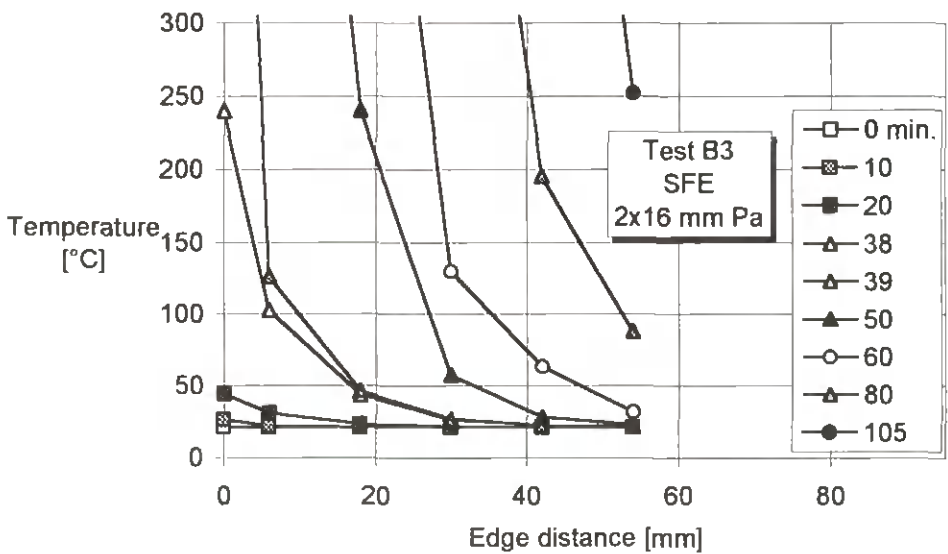
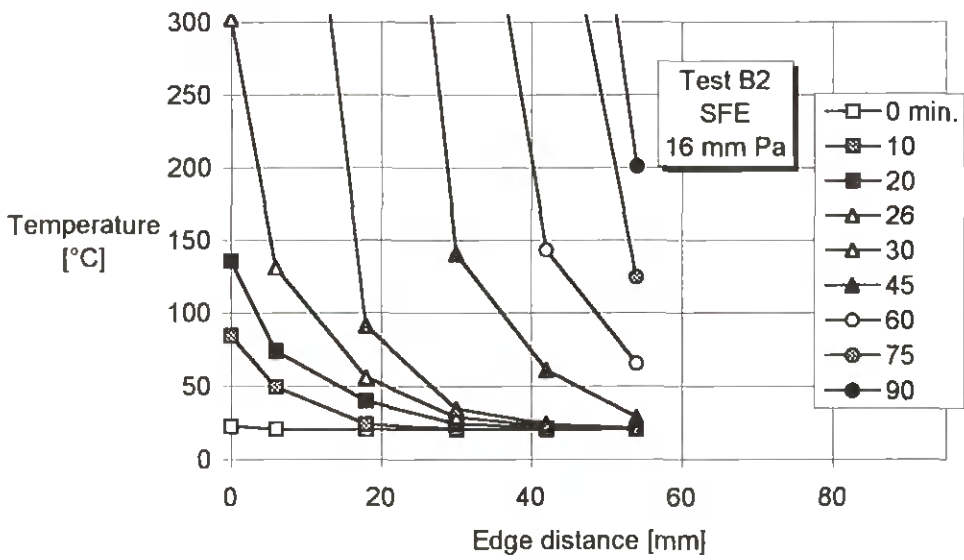
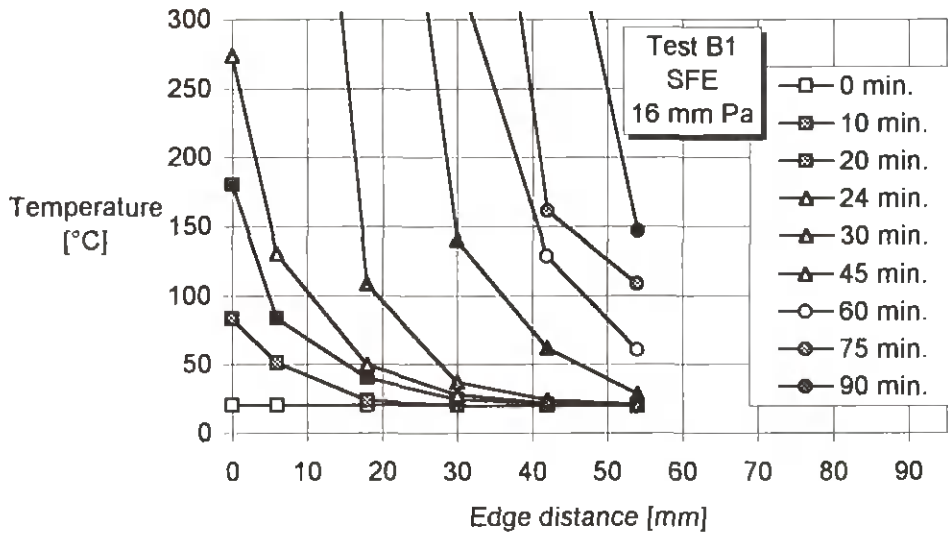


Figure 2.16: Temperature profiles in members of tests B1-B3 (initially protected member)

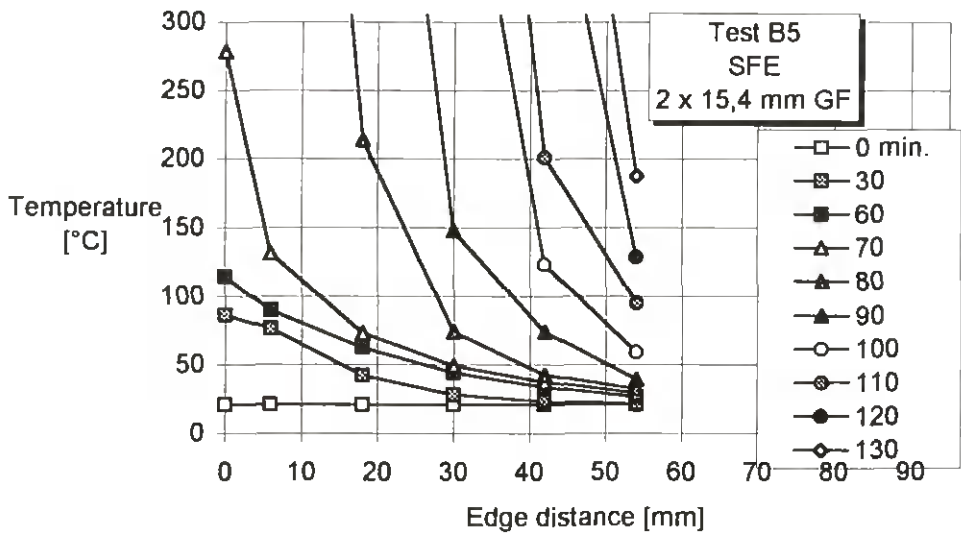
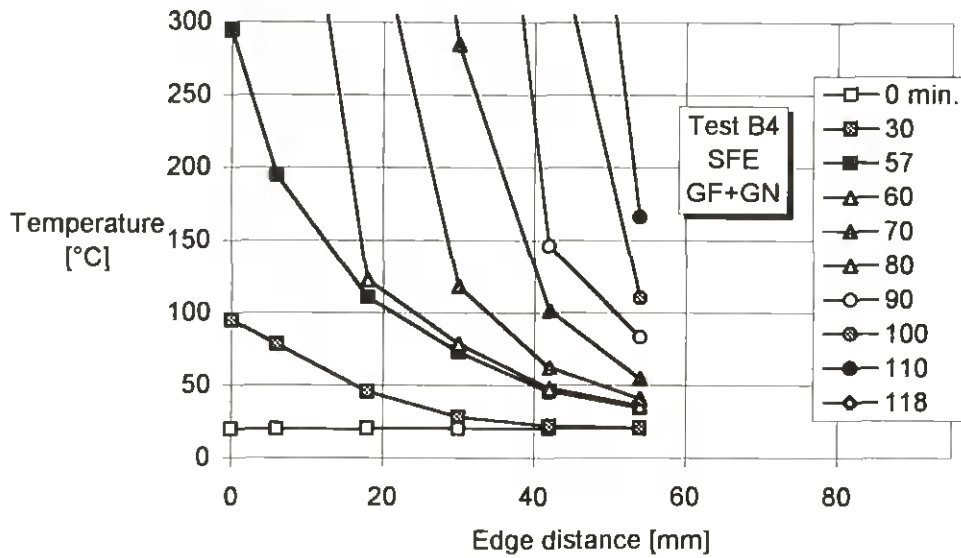


Figure 2.17: Temperature profiles in members of tests B4 and B5 (initially protected member)

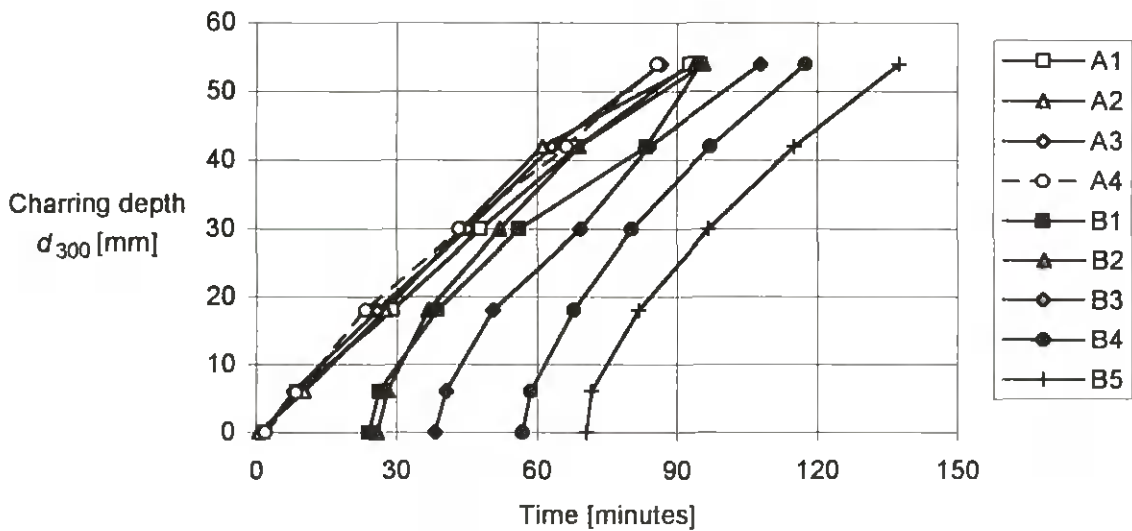


Figure 2.18: Charring depths versus time of series A and B

2.5 Series C: Parametric fire exposure of initially unprotected timber

In general, the target curves are characterized by a fast temperature rise in the beginning, followed by a plateau-like phase where the temperature increases slowly and finally by the decay phase with a shape similar to an exponential function. In all tests the equipment did not allow to follow the target curves in the beginning and to reach the plateau temperature in due time. In tests C1-C3, during the first stage of increasing temperature, the temperature followed the standard fire curve rather than the target curve, see Figure 2.19

In tests C4-C6 the temperature deviations were considerable. Firstly, the temperature followed a curve similar to a factored standard fire curve, and secondly, in two of the tests the maximum temperature was much lower than given by the target curve. Two parametric fire curves were found in order to fit the experimental curves of test C4 and C6, in order to be used in 3.3 for comparison of the charring depths given by the Fire Part of Eurocode 5¹ with test results, see Figure 2.20.

The recorded temperature-time relationships are shown in Figure 2.21 and 2.22. Temperature profiles in the member are shown in Figure 2.23 and Figure 2.24.

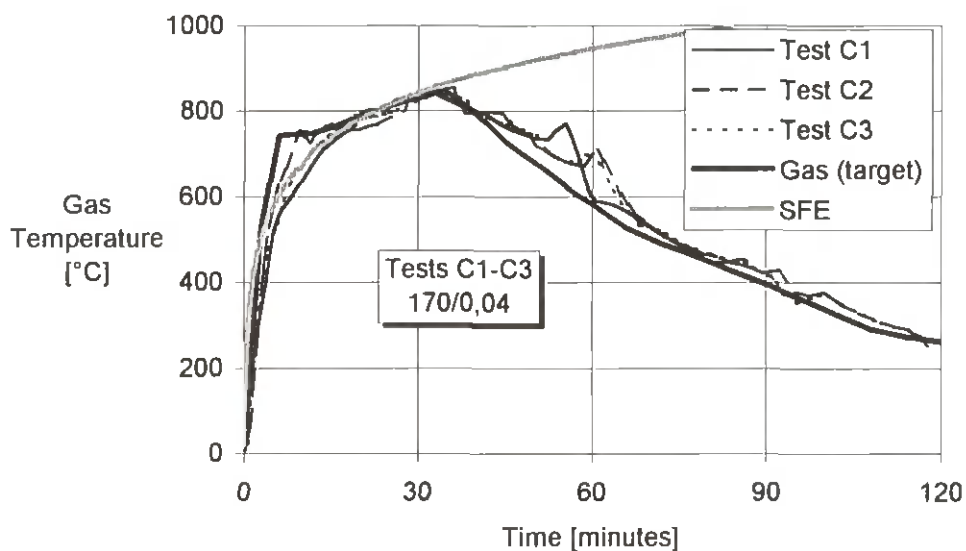


Figure 2.19: Comparison of gas temperature-time curves with target fire curve and standard fire curve

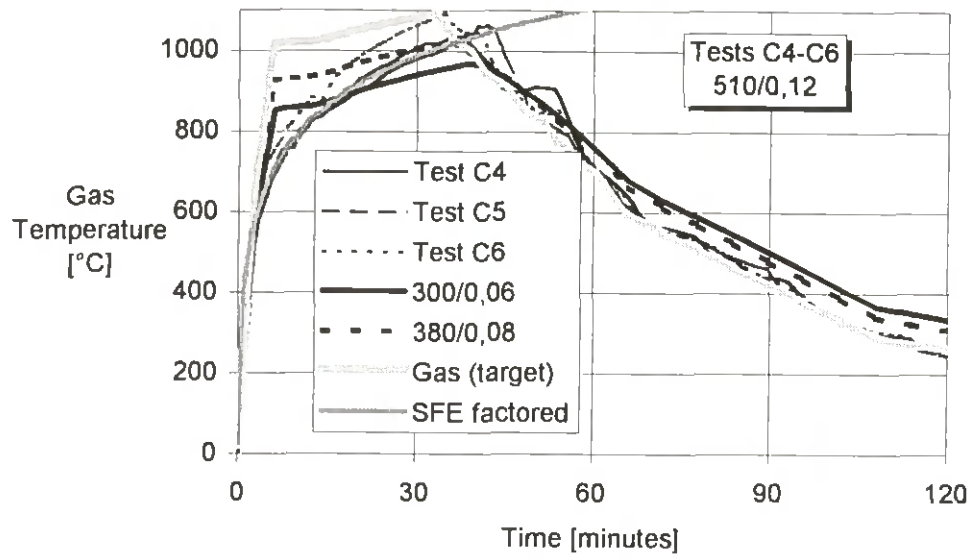


Figure 2.20: Comparison of gas temperature-time curves with target fire curve and fitted parametric fire curves

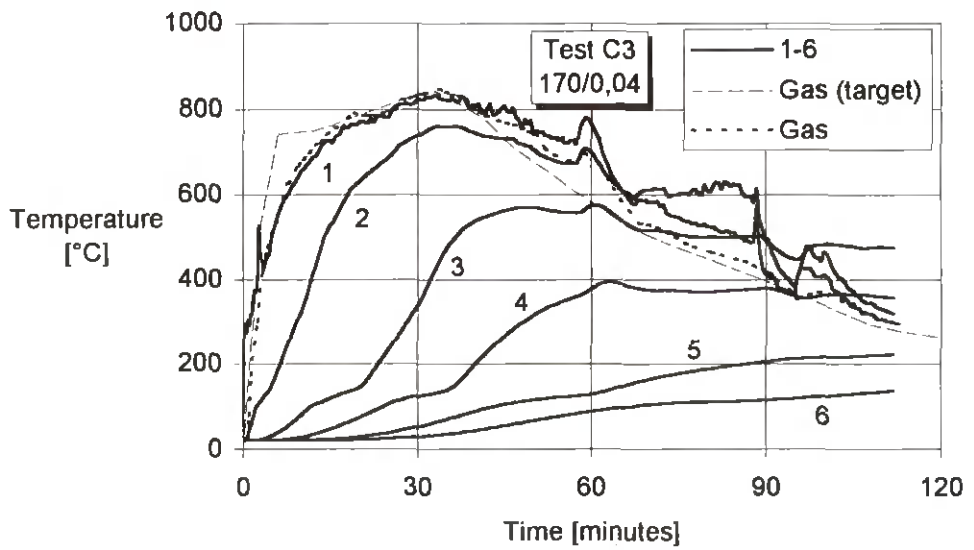
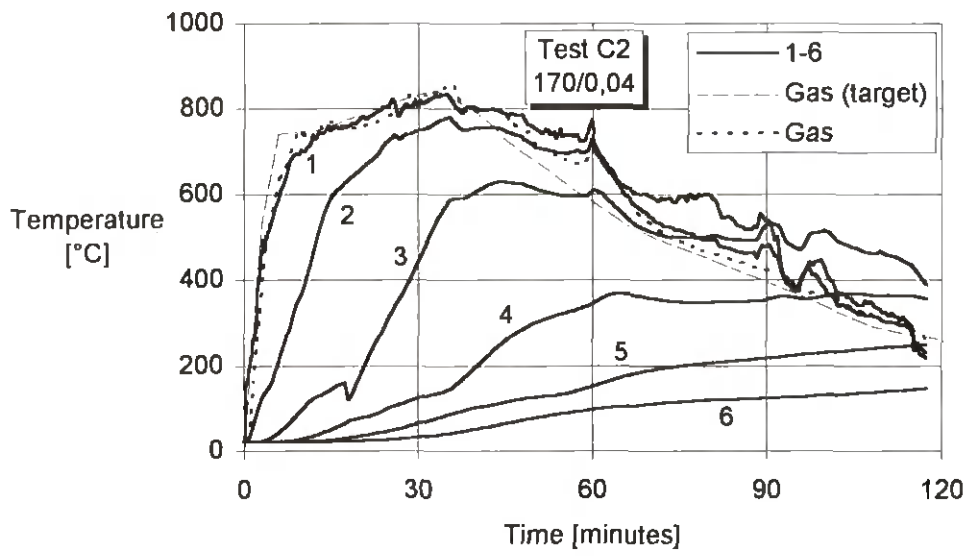
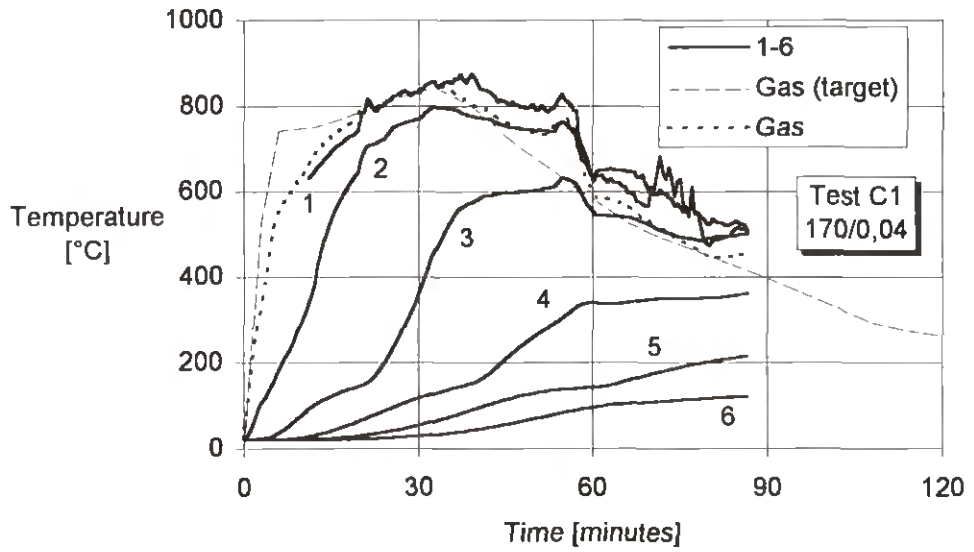


Figure 2.21: Temperature-time relationships of tests C1-C3

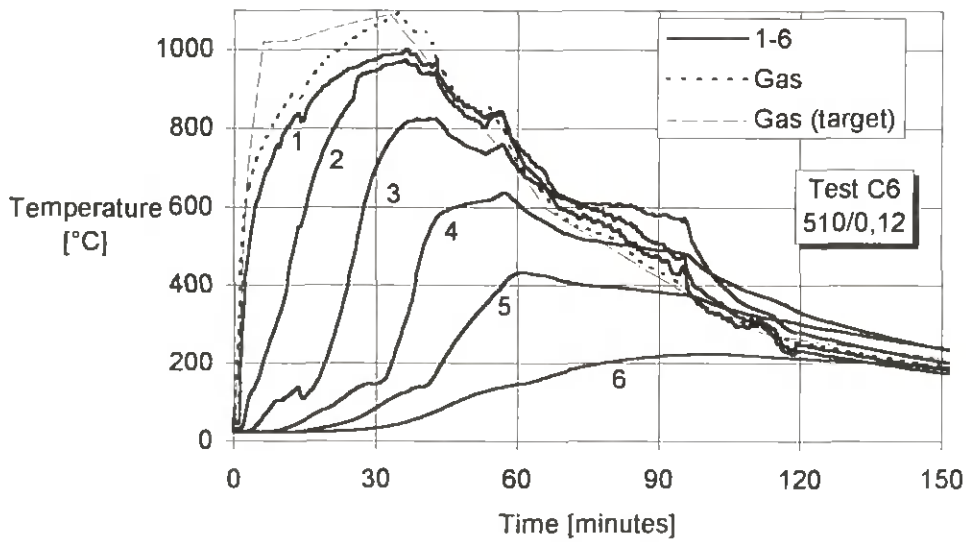
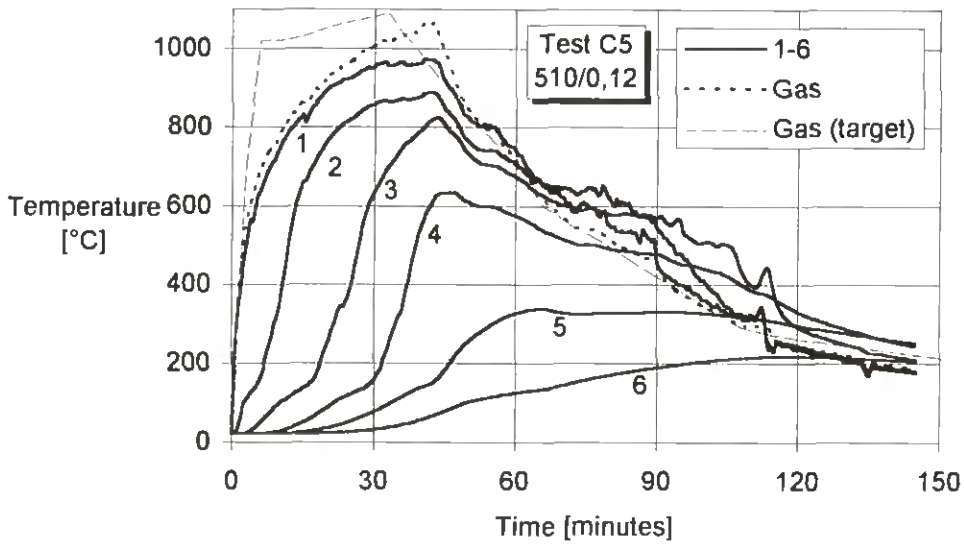
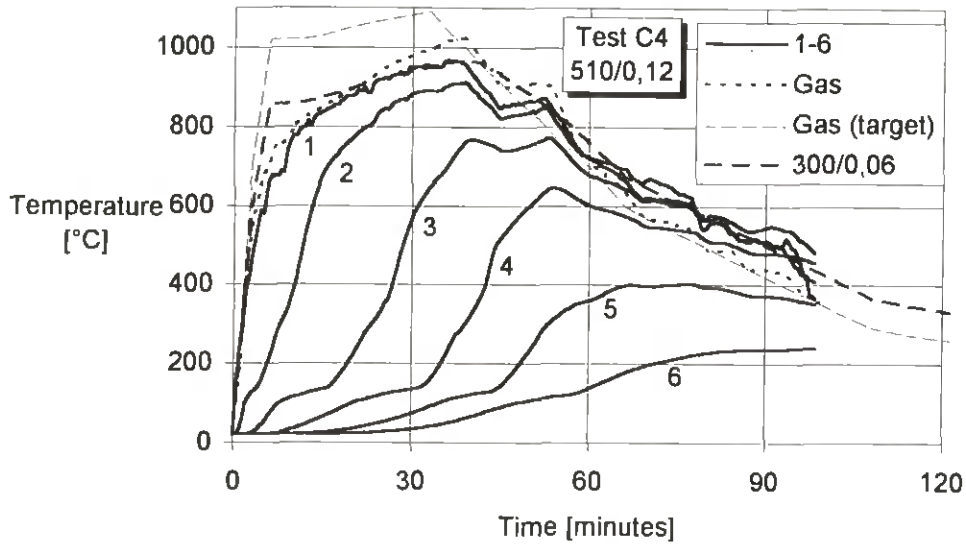


Figure 2.22: Temperature-time relationships of tests C4-C6

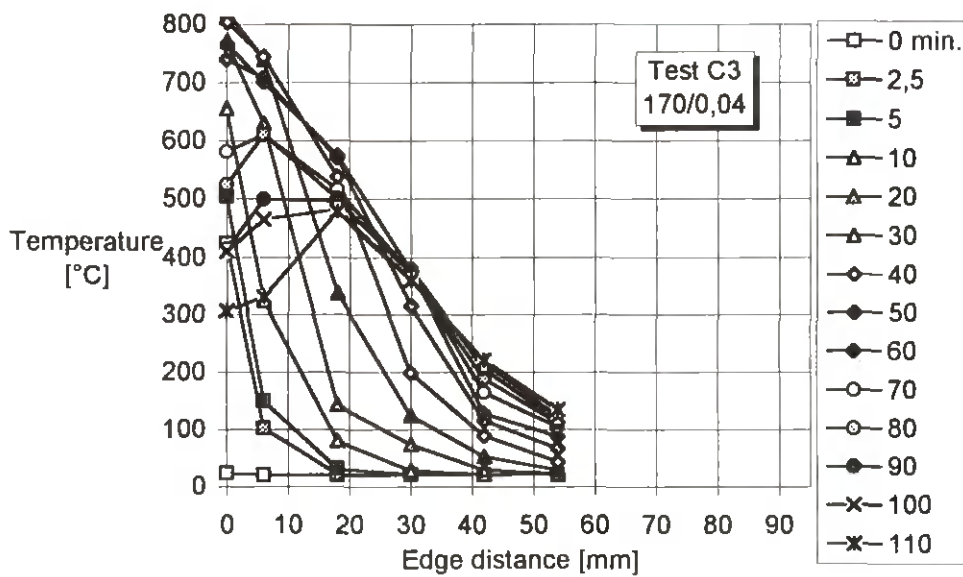
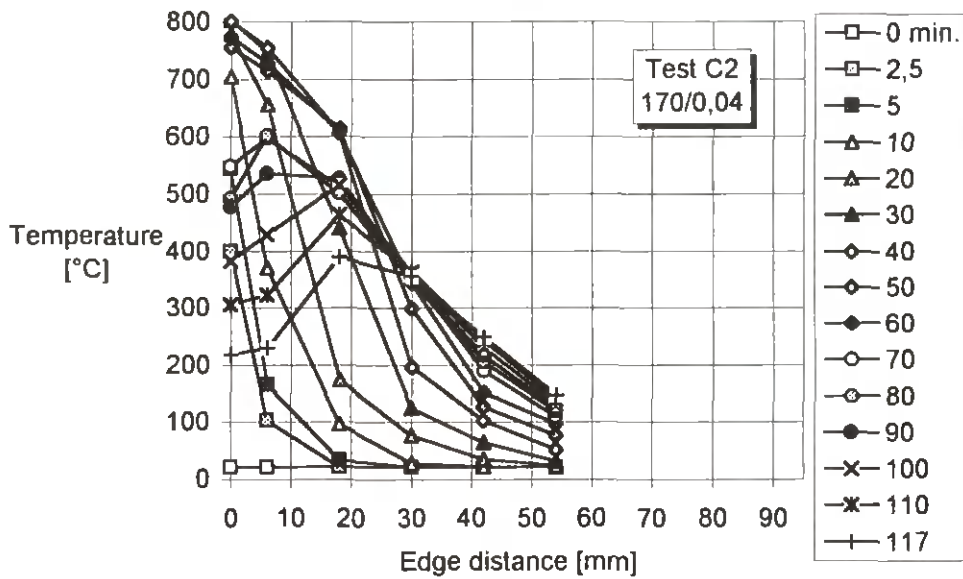
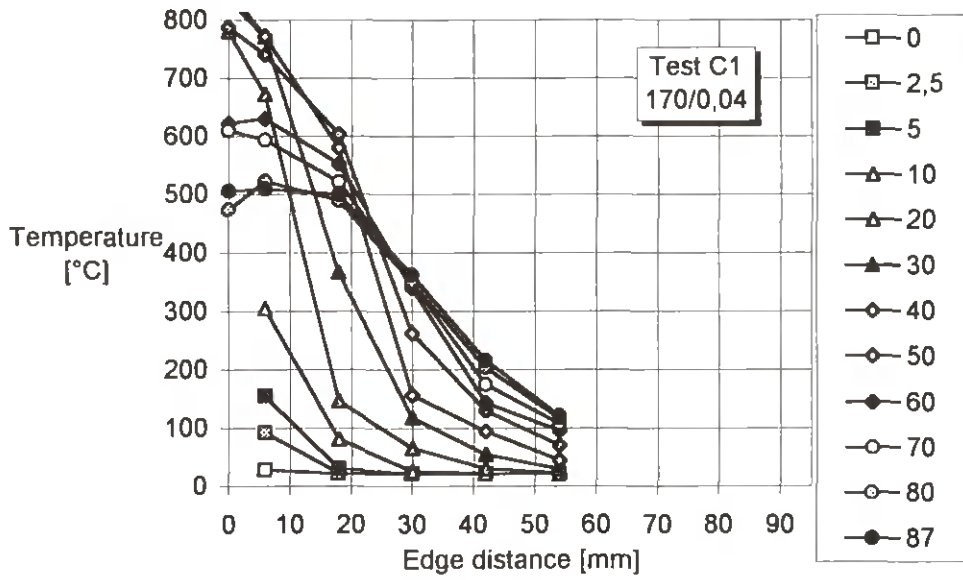


Figure 2.23: Temperature profiles of tests C1-C3

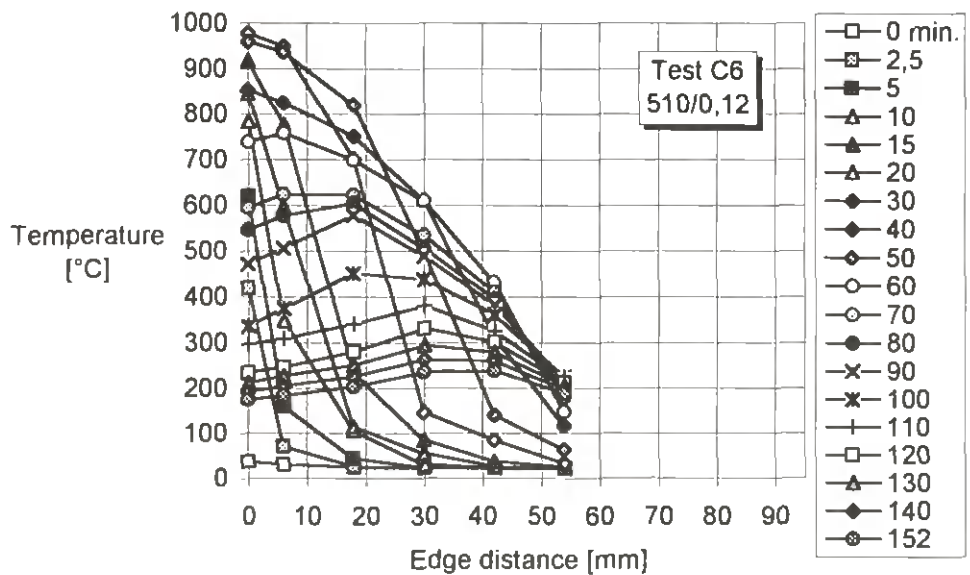
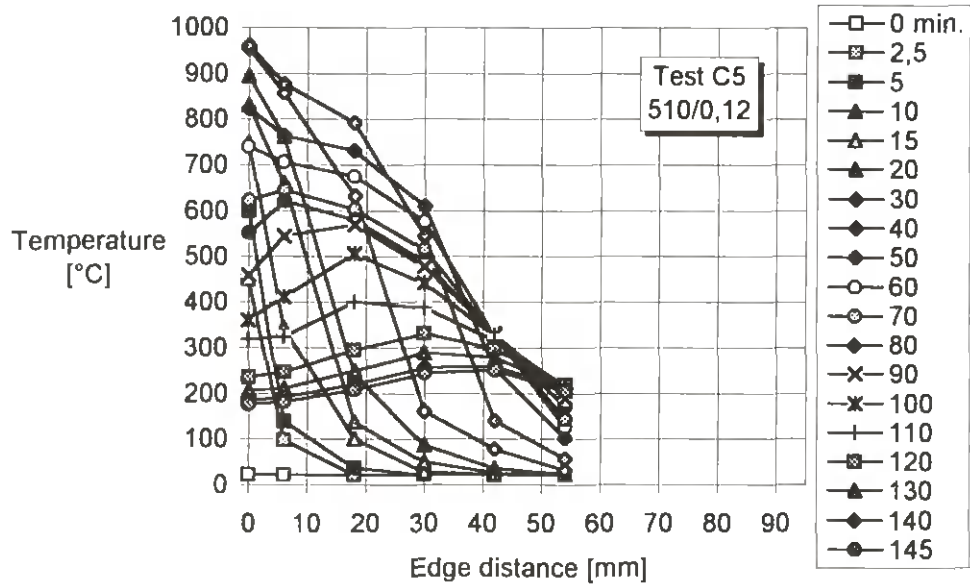
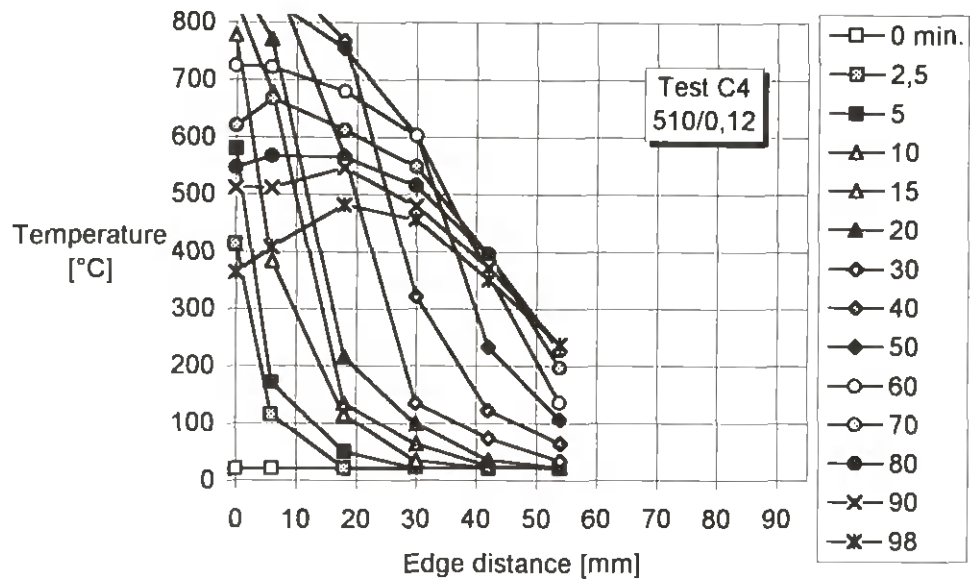


Figure 2.24: Temperature profiles of tests C4-C6

The propagation of the char-line is shown as the position of the 300-degree isotherm, see Figure 2.25 and 2.26. In tests C1-C3 the propagation of the charring depth was measured directly up to a charring depth of 30 mm at gauge point 4. Beyond that depth, the position of the 300-degree isotherm was found by linear interpolation, i.e. by determining the intersection of the temperature profile between the edge distances 30 and 42 mm, see Figure 2.23. We can see that the charring depth reaches a maximum of about 33 to 37 mm. For tests C4-C6 this was done correspondingly for charring depths greater than 42 mm.

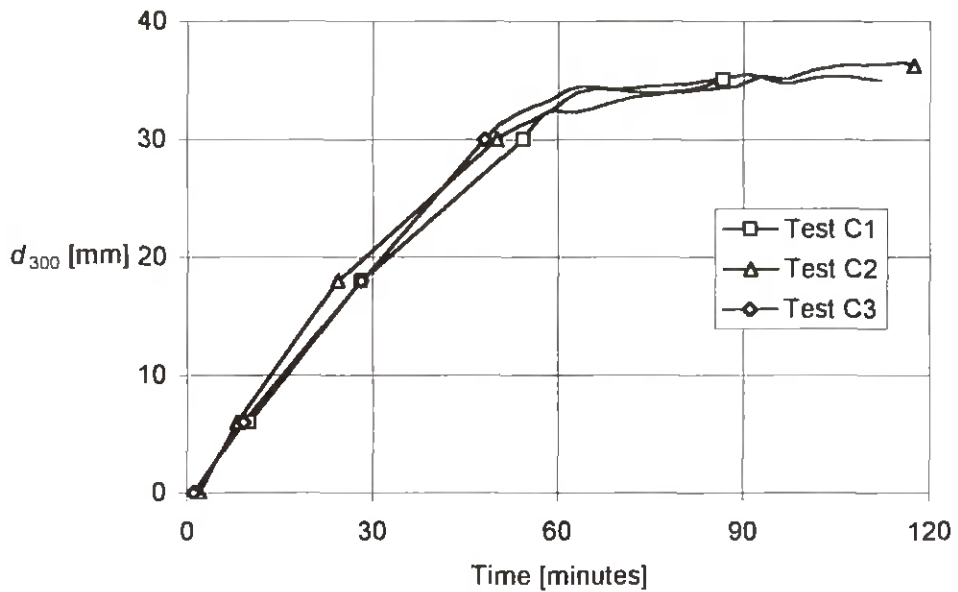


Figure 2.25: Charring depths versus time of specimens C1-C3

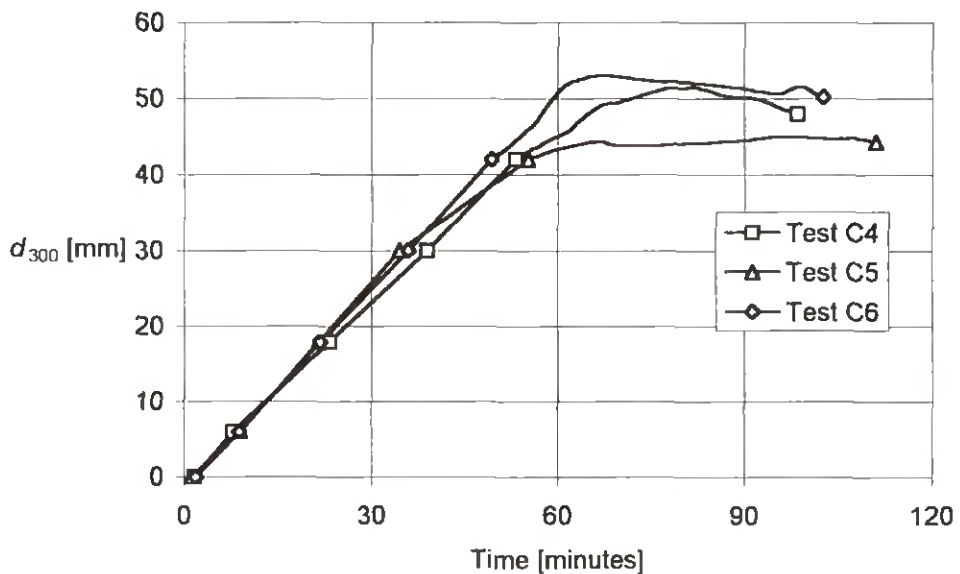


Figure 2.26: Charring depths versus time of specimens C4-C6

3 Modelling

3.1 General

In order to determine the progress of the char-line, the computer program TEMPCALC⁷ was used, developed for the calculation of heat transfer using the Finite Element Method. The computer program solves the two-dimensional, transient, heat transfer differential equation incorporating thermal properties that vary with temperature. Mass transfer is not taken into account. Assemblies comprising several materials can be analysed and the heat absorbed by any existing void cavities in the assembly is also taken into account.

The structure is modelled by rectangular finite elements using a mesh consisting of boundary, horizontal and vertical lines. The thermal properties of the materials are defined by polynomials of conductivity and heat capacity versus temperature. Time dependent input values for convection and emissivity are included. In the calculations reported here, the convection coefficient γ was taken as $25 \text{ Wm}^{-2}\text{K}^{-1}$ and the emissivity coefficient ε was taken as 0,56.

The temperature at the boundaries of the structure is given by a time-temperature curve. The heat transferred by convection and radiation at the boundaries are modelled as functions of time.

A general problem when using analytical models to calculate the heat transfer through structures is that, due to simplifications and deficiencies of the model, the thermal properties of the materials used as input parameters must be calibrated such that the results are fitted to those obtained by tests. Deviations from the real test conditions may be necessary since the model used by TEMPCALC does not take into account the

- mass transfer within the structure
- reaction energy released inside the wood due to pyrolysis
- degradation of material, e.g. the cracking of char coal which increases the heat transfer of the char layer.

The influence of mass transfer is most pronounced at temperatures around 100°C when water is evaporated and transported further into the wood where the vapour condenses into water again. The magnitude of heat of reaction has been discussed by several authors^{8,9,10}, however its effect is usually ignored. In the following, the results of the calibration are shown in relation to data reported by other authors.

3.2 Calibration of material properties

3.2.1 Standard fire exposure

Some examples of thermal conductivity values of wood from other sources, Thomas¹¹, Fredlund^{12,13}, Knudson et al.¹⁴ and Janssens¹⁵, are shown in Figure 3.1. Fredlund uses one curve for wood and one curve for charcoal. The figure shows his data for temperatures below 300°C and for charcoal for temperatures above 300°C . Knudson et al. give values for wood for temperatures up to 200°C and for charcoal from 350°C and assume a linear relationship between these temperatures describing the effect of thermal decomposition of wood. The values by Harmathy are taken from Thomas. Janssens gives a set of expressions for the

determination of conductivity values. The values shown in the graph were determined by Thomas evaluating these expressions. Thomas simulates the effect of the evaporation of water, the transport of vapour into the wood and the condensation by assuming a considerable increase of conductivity between 60 and 110°C.

The time-conductivity relationship obtained in this study by calibration to the experimental results reported in 2.3 deviates from the other curves mainly for high temperatures, see Figure 3.1 and Table 3.1. This deviation is discussed below. Using higher conductivity values below 100°C and lower ones between 100°C and 300°C in order to model the effect of energy transport by vaporising of water did not give better results.

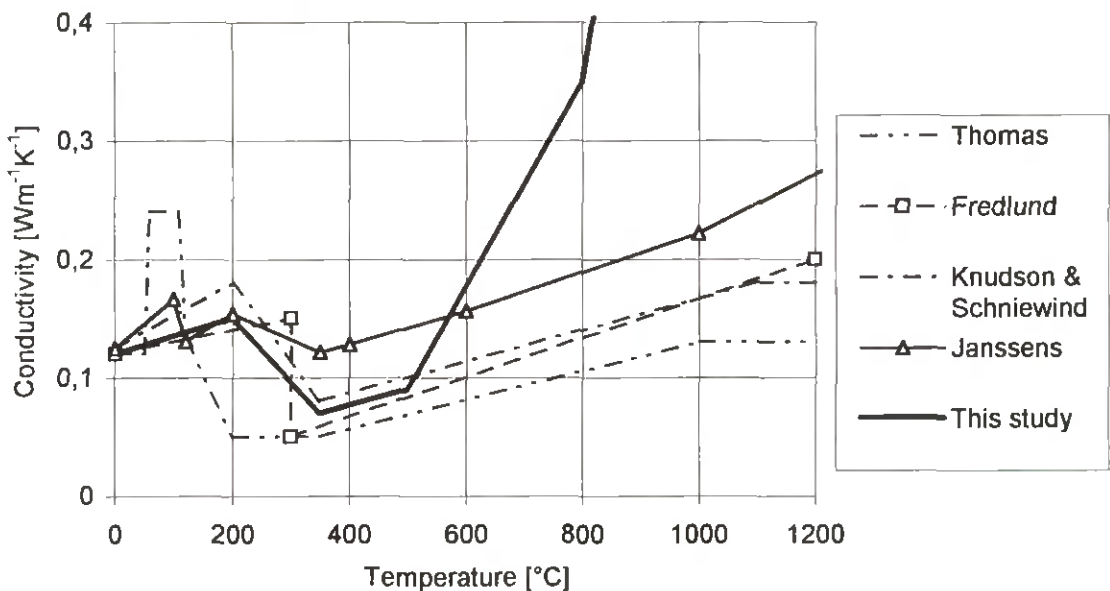


Figure 3.1: Thermal conductivity values for wood.

Relationships of specific heat versus temperature from other sources by Mehaffey¹⁰, Knudson et al.¹⁴, Janssens¹⁵, Gammon¹⁶, Landolt-Börnstein¹⁷ (referenced by Fredlund¹³) and Widell¹⁸ (referenced by Janssens¹⁵), are shown in Figure 3.2. The values adopted by ENV 1995-1-2 agree with those of Mehaffey et al. in the region from 20°C to 200°C, and with the values according to Landolt-Börnstein given for charcoal.

The peak of the curves at 100°C depends on the energy needed to evaporate water inside the wood, causing a delay of temperature rise above 100°C in the wood, see Figure 3.3. Mehaffey et al. assume that pyrolysis is endothermic and that energy is consumed in the region between 200 and 350°C, see Figure 3.2. They assume that the heat absorbed is $q = 370$ J/g. This value from Tang et al.¹⁹ as referenced by Roberts⁹ is, however, the energy absorbed per unit mass of volatile products rather than per unit mass of wood initially present as in the assumption by Mehaffey et al.

The resultant values of specific heat obtained in the calculations of this study shown in Figure 3.2 and Table 3.2, follow approximately the relationship given by Mehaffey regarding the peak values around 100°C. As a minor modification, however, the heat capacity of wood is assumed to decrease linearly to zero between 800°C and 1200°C, simulating that at approximately

1000°C charcoal is consumed at the same rate as the char line propagates into the wood (Fredlund²⁰).

Table 3.1: Temperature-conductivity relationship for wood used in this study

Temperature °C	Conductivity Wm ⁻¹ K ⁻¹
0	0,12
200	0,15
350	0,07
500	0,09
800	0,35
1200	1,50

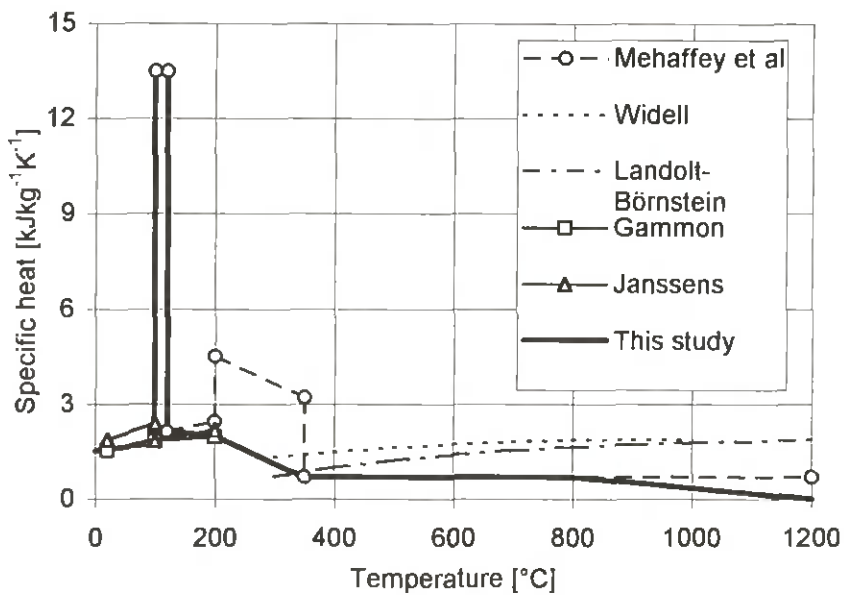


Figure 3.2: Specific heat values of wood

During the process of calibration, contrary to the assumption made by Mehaffey, between 200°C and 450°C the reaction during the pyrolysis of the wood was assumed to be exothermic. Using the data given by Roberts⁹, the mean heat of reaction was assumed to be $Q = -180 \text{ J/g}$ and the reaction to take place in this temperature interval. The resultant reduction of specific heat by $0,72 \text{ kJ kg}^{-1} \text{ K}^{-1}$ between 200°C and 450°C did not affect the results significantly. Therefore, the heat of reaction during pyrolysis not taken into account, irrespective of whether the reaction is endothermic or exothermic.

In order to determine specific heat related to thickness instead of mass, the densities given in Table 3.2 were used.

Figure 3.3 shows the calculated time-temperature curves for specific locations in the member in comparison with the data of tests A1-A4 given in 2.3. The calculated time-temperature curves show good agreement with the data obtained in the fire tests.

Table 3.2: Specific heat and densities used in this study

Temperature °C	Specific heat kJ kg ⁻¹ K ⁻¹	Density kg/m ³
20	1,52	480
100	1,76	480
100	13,5	480
120	13,5	425
120	1,64	425
200	2,00	425
200	1,28	425
350	0,00	300
450	0,00	300
450	0,69	300
800	0,69	300
1000	0,69	300
1200	0	0

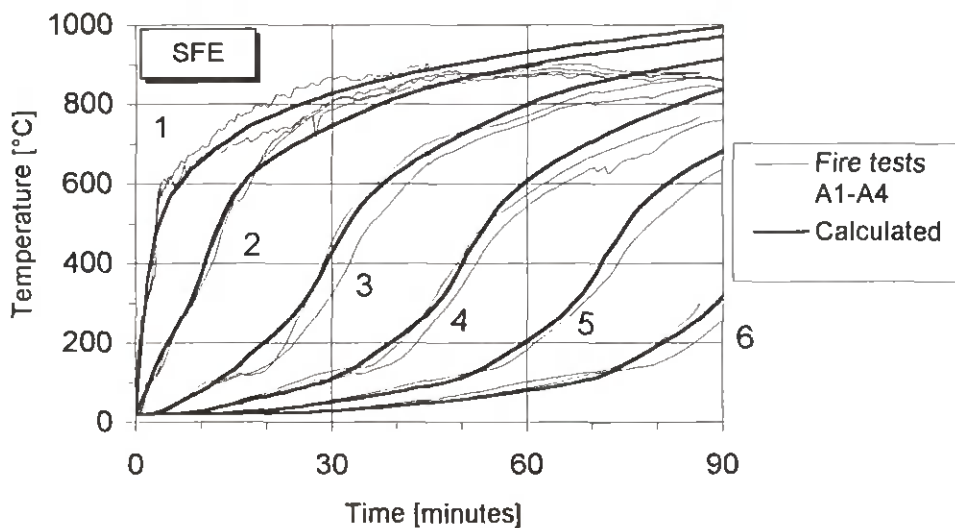


Figure 3.3: Temperature-time relationships of tests A1-A4: Comparison of fire tests and calculations

The calculated propagation of the char-line is in good agreement with the experimental results, see Figure 3.4. The calculated charring rate, defined as secant values, is shown in Figure 3.5 as a function of time in comparison with the experimental heat curves as shown above in Figure 2.14.

The assumed conductivity of the char-layer, i.e. the conductivity for temperatures of more than 350°C deviates considerably from values from most other sources for temperatures of more than 600°C. The effect of this deviation can be seen from Figure 3.6. Using the data according to Fredlund for temperatures exceeding 500°C, the calculated charring depths deviate considerably from the experimental ones. This is probably caused by the fact that the char layer is cracking such that the heat passing through the char layer is increased. Fredlund²⁰ reports that charcoal starts glowing at 500°C, and it is therefore assumed that cracking start around

that temperature. For temperatures greater than 500 the conductivity values relate to the char layer (including cracks) rather than to charcoal.

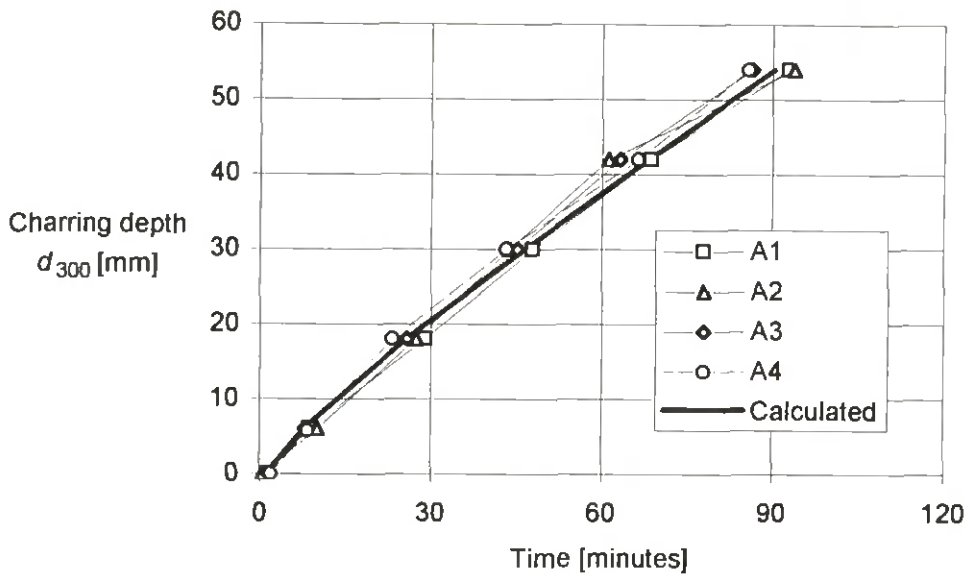


Figure 3.4: Charring depths versus time: Comparison of experimental curves with calculated values

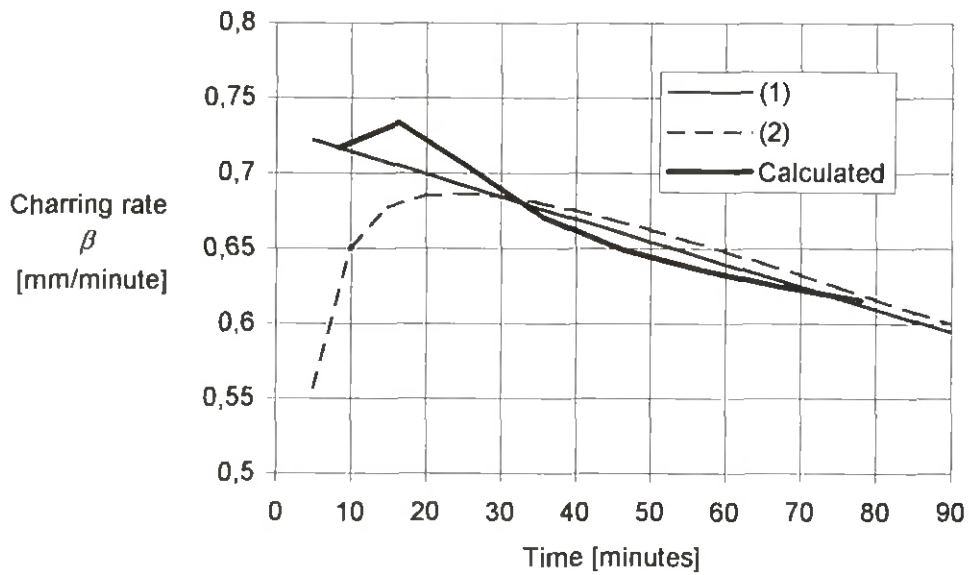


Figure 3.5: Charring rate (secant value) versus time: Comparison of calculated with experimental curves

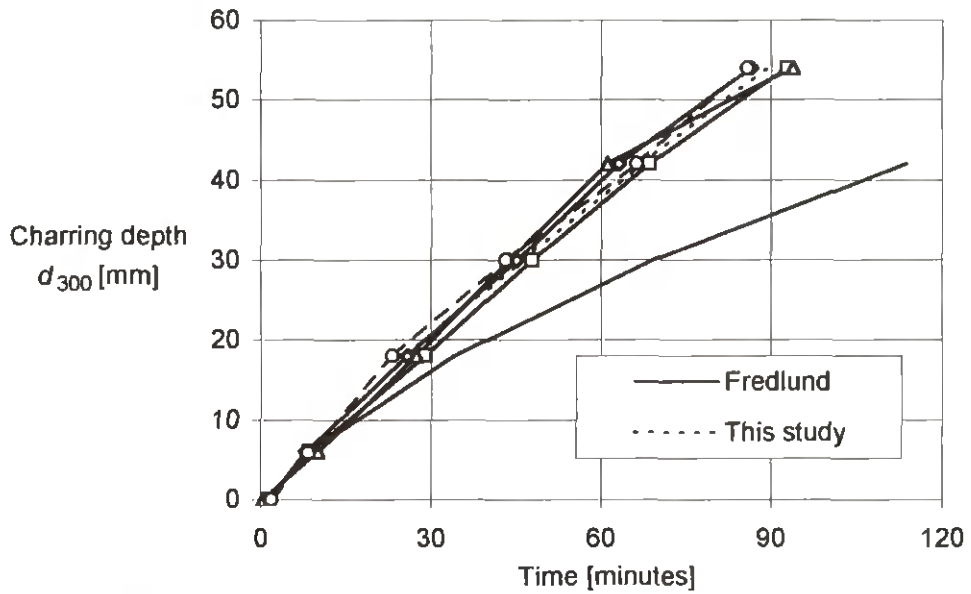


Figure 3.6: Charring depth versus time: Effect of assumed conductivity of char layer according to this study and Fredlund

Using the material properties obtained by calibration to the experimental results of series A (initially unprotected wood), charring depths were calculated for initially protected wood corresponding to series B, see Figure 3.7.

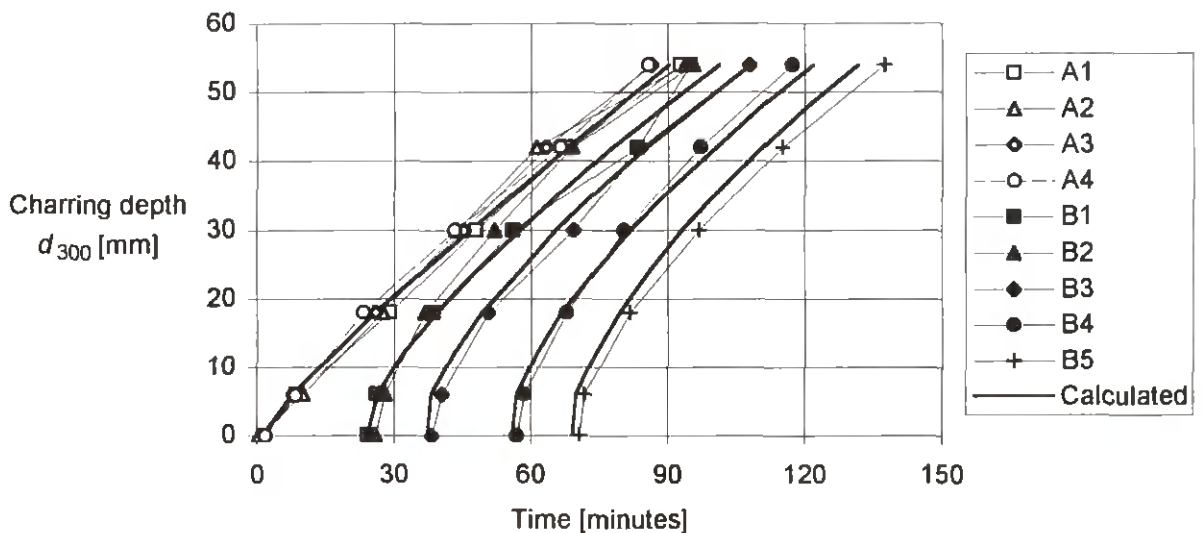


Figure 3.7: Charring depths versus time: Comparison of experimental curves with calculated values for series A and B

The calculations were performed by simulating the effect of initial protection using the following procedure: The computer program was run “unprotected” following the standard time-temperature curve, however with a ten-fold time scale. When the surface temperature of the member reached 300°C, the gas temperature was immediately increased to the value of the standard time-temperature curve corresponding to time of onset of charring observed in the

fire tests. From that time the gas temperature followed the real standard time-temperature curve. The agreement between the shapes of calculated and experimental curves is fairly good.

Contrary to the time-charring depth relationship for initially unprotected surfaces, in the case of retarded onset of charring the relationships are pronounced non-linear. For design purpose, the non-linear curves should be replaced by a linear or bi-linear model, the latter preferably for large charring depths in order to prevent too conservative results.

In Figure 3.8 linear and bi-linear relationships are shown in comparison with calculated ones. For initially protected surfaces, the slope of the linear curves was put equal to the secant value at the charring depths of 15 mm, while the slope of the second part of the bi-linear curves was put equal to the secant value between the charring depths 15 and 40 mm.

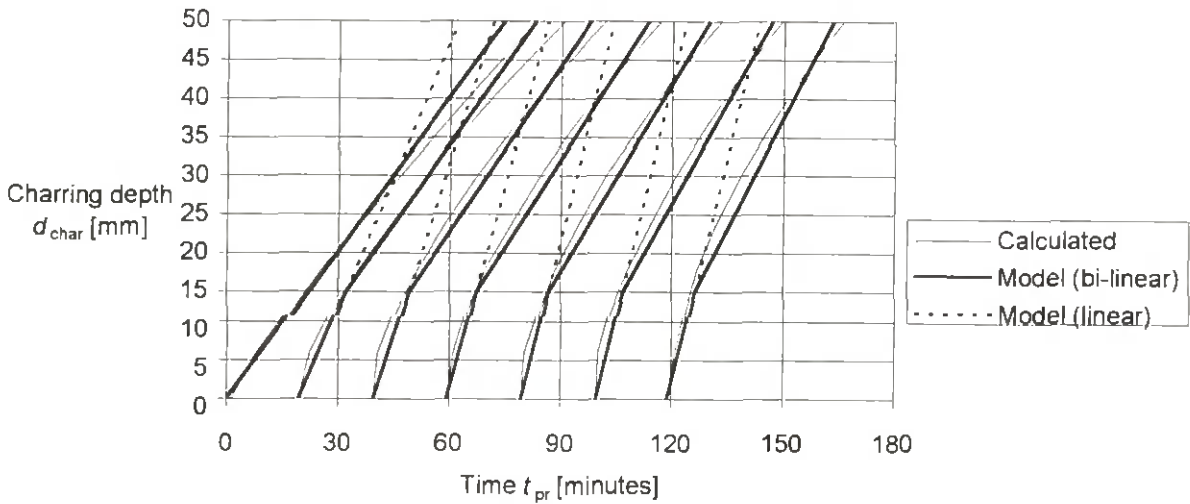


Figure 3.8: Comparison of linear and bi-linear model with calculated relationships between time and charring depth

Defining the ratios of charring rates for initially unprotected and protected surfaces as

$$\kappa_1 = \frac{\beta_1}{\beta_0} \quad (3.1)$$

and

$$\kappa_2 = \frac{\beta_2}{\beta_0} \quad (3.2)$$

where

β_1 is the charring rate of initially protected surfaces according to the linear model or the first stage of the bi-linear model,

β_2 is the charring rate of initially protected surfaces according to the second stage of the bi-linear model,

and putting the charring rate of initially unprotected surfaces as $\beta_0 = 0,67$ mm/minute, we get the following relationships (see Figure 3.9):

$$\kappa_1 = -0,000151 t_{pr}^2 + 0,0409 t_{pr} + 1 \quad (3.3)$$

$$\kappa_2 = 0,0000231 t_{pr}^2 + 0,00103 t_{pr} + 1 \quad (3.4)$$

where t_{pr} is the time of onset of charring.

The values were determined from the calculated relationships between time and charring depth and fitted by polynomials. The scatter of the values was caused by numerical deviations running the computer program.

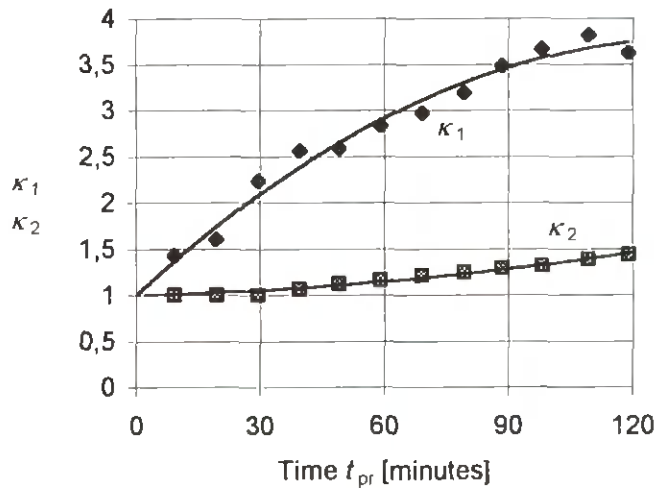


Figure 3.9: Ratio of charring rates for linear and bi-linear model versus time of onset of charring

3.2.2 Parametric fire exposure

Using the same thermo-physical properties of wood and charcoal when modelling parametric fires as when modelling heat transfer at standard fire exposure, see 3.2.1, we get the time-temperature relationships shown in Figure 3.10. The input fire curve used in the calculation was approximately equal to the mean curve of the gas temperature recorded during the tests.

The calculated values of temperature in the member are in good agreement in the beginning; during the decay phase. The calculated curves do, however, not reach the peak temperatures recorded during the tests.

In order to obtain better agreement between tests and calculation, a fictitious fire curve was used by assuming higher temperatures during the decay phase by increasing the nominal fire load density of 170 MJ/m^2 by 50 MJ/m^2 . The calculated temperatures were now in better agreement. This can also be seen from the comparison of charring depths, see Figure 3.12.

Even though the prediction of charring depth is good using the modified fire curve, the temperature profiles in the member do not agree well with the experimental curves, c.f. Figure 3.13 and 2.23. In the calculations, the reverse temperature gradient observed in the tests is not

predicted. Contrary to the test results, the gas temperature used in the calculation is always greater than the calculated surface temperature of the member.

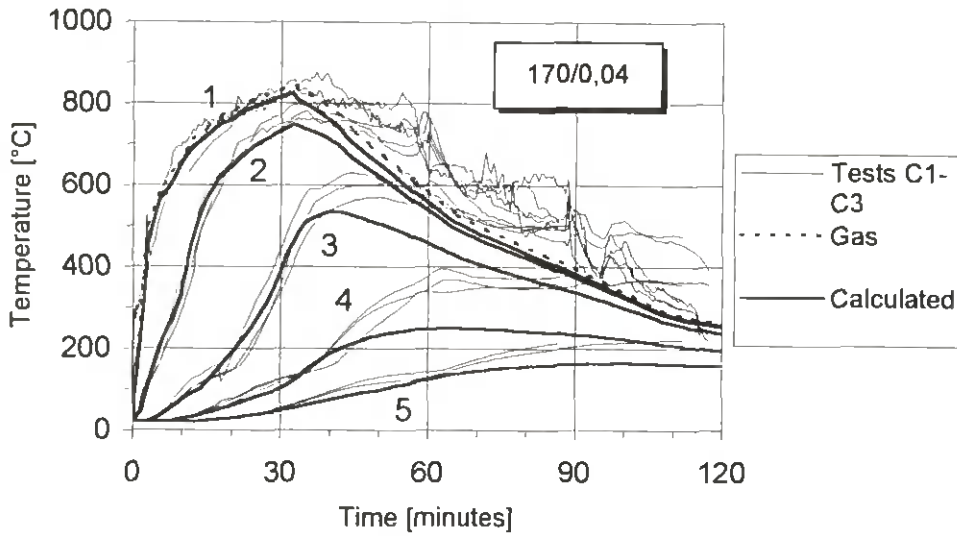


Figure 3.10: Time-temperature relationships of tests C1-C3: Comparison of fire tests and calculations using the same thermal properties as for standard fire exposure

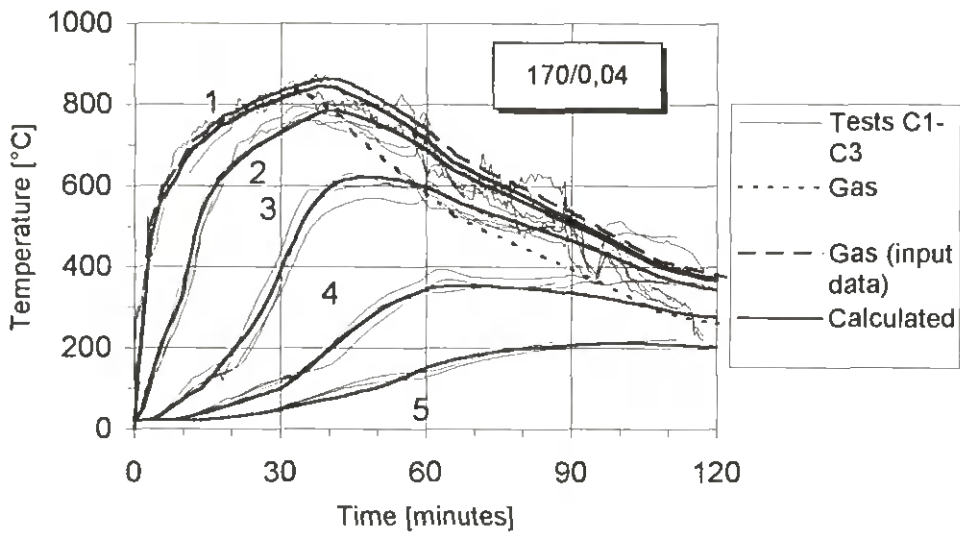


Figure 3.11: Time-temperature relationships of tests C1-C3: Fitted calculated results by using fictitious temperature during the decay phase

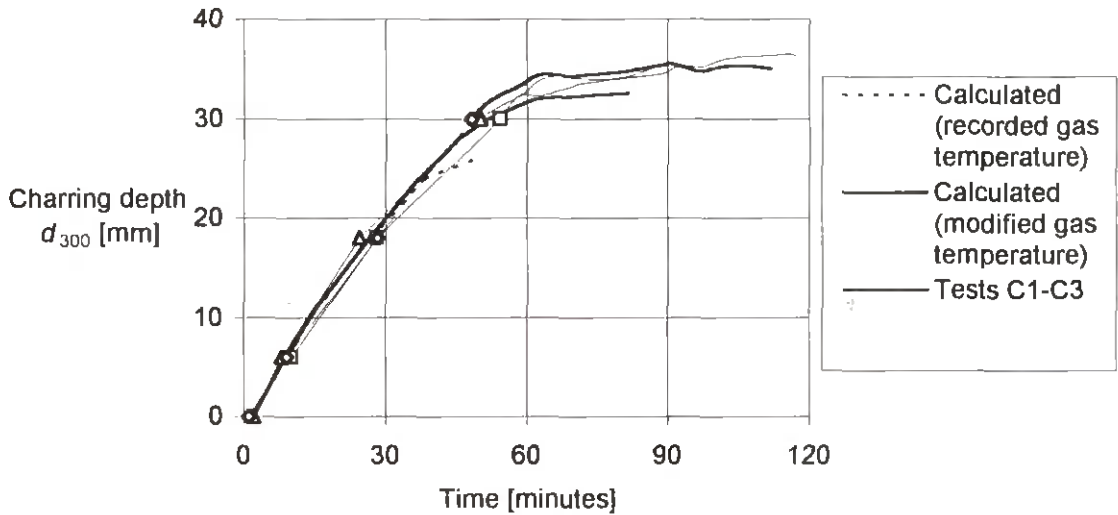


Figure 3.12: Charring depths versus time: Comparison of experimental curves with calculated values

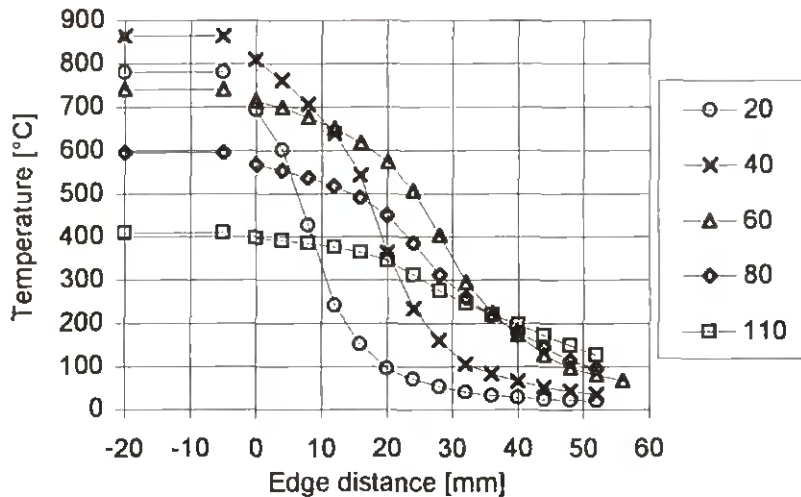


Figure 3.13: Calculated temperature profiles for specified times using the modified fire curve for tests C1-C3

The results of calculations using material properties from clause 3.2.1 applied to tests C4-C6 are similar to those for tests C1-C3 shown in Figure 3.10. Again, a fictitious fire curve was used by increasing the temperature during the decay phase, corresponding to a fictitious increase of the fire load density by 50 MJ/m^2 . The results of the calculations are shown in Figure 3.14 and 3.15. In the calculations, the temperature rise is greater than in the tests, however the prediction of the maximum charring depth is fairly good.

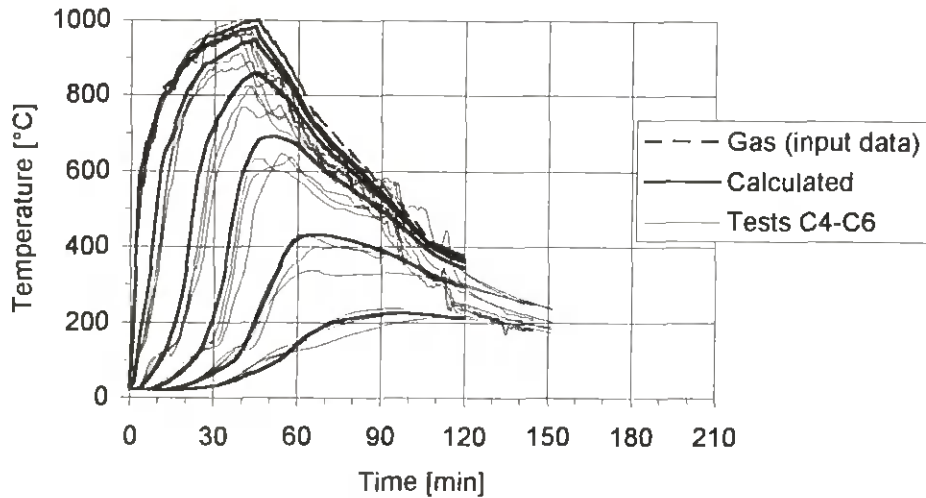


Figure 3.14: Time-temperature relationships of tests C1-C3: Fitted calculated results by using fictitious temperature during the decay phase

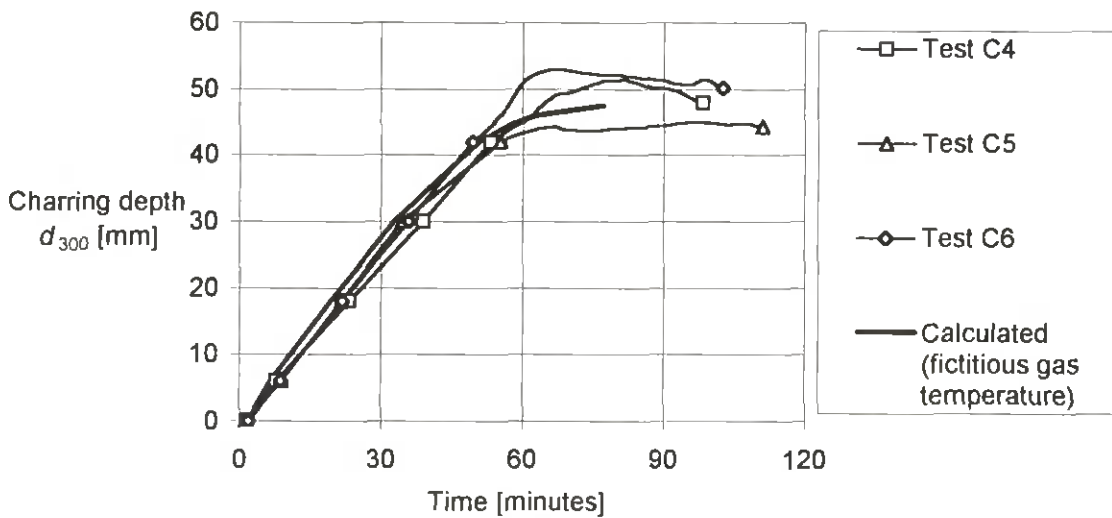


Figure 3.15: Charring depth versus time for parametric curve 510/0.12: Comparison of experimental tests and calculations using a fictitious fire curve during the decay phase

It is argued that a better agreement between calculation and test results can be obtained by calibrating the thermal properties of the char layer and wood during the decay phase. Unfortunately, TEMPCALC does not allow varying input parameters for different stages of the complete fire endurance.

It was also tried, however without success, to assume a heat source by using negative specific heat values in the pyrolysis zone. The negative effect of this manipulation was that the charring rate increased considerably above the test results.

The prediction of charring depth during the first stage of the fire exposure is better for fire curves determined for an opening factor of $0,04 \text{ m}^{1/2}$ (corresponding to the standard fire curve). The calculations indicate that the material properties used for standard fire exposure

give a poorer prediction for opening factors greater than $0,04 \text{ m}^{1/2}$. This prediction is however conservative. The thermal properties of wood and the char layer should be calibrated further in order to reach better agreement with the test results.

3.3 Charring depth at parametric fire exposure according to Eurocode 5

Based on the work by Hadvig²¹ and Bolonius Olesen et al.²² in the Fire Part of Eurocode 5¹ charring of wood exposed to parametric fires is described in time steps of t_0 , see Figure 3.16, of

$$t_0 = 0,006 \frac{q_{t,d}}{O} \quad (3.5)$$

where $q_{t,d}$ is the fire load density related to the total area of floors, walls and ceilings of the enclosure of the fire compartment in MJ/m^2 and O is the opening factor in $\text{m}^{1/2}$.

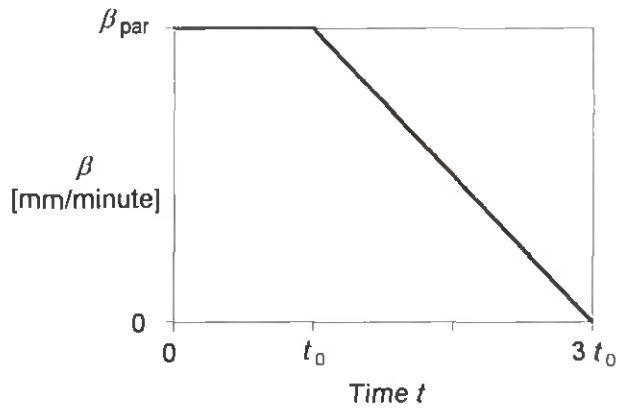


Figure 3.16: The charring rate of wood at parametric fire exposure according to Eurocode 5

The maximum charring rate β_{par} is given as

$$\beta_{\text{par}} = 1,5\beta_0 \frac{50 - 0,04}{4O + 0,08} \quad (3.6)$$

where β_0 is the charring rate at standard fire exposure.

The charring depth is

$$d_{\text{char}} = \beta_{\text{par}} t \quad \text{for } 0 \leq t \leq t_0 \quad (3.7)$$

$$d_{\text{char}} = \beta_{\text{par}} \left(t - \frac{(t - t_0)^2}{4 t_0} \right) \quad \text{for } t_0 \leq t \leq 3 t_0 \quad (3.8)$$

with a maximum value given as

$$d_{\text{char,max}} = 2 \beta_{\text{par}} t_0 \quad (3.9)$$

In Figure 3.17 these expressions are compared with the results of tests C1-C3. The agreement is fairly good.

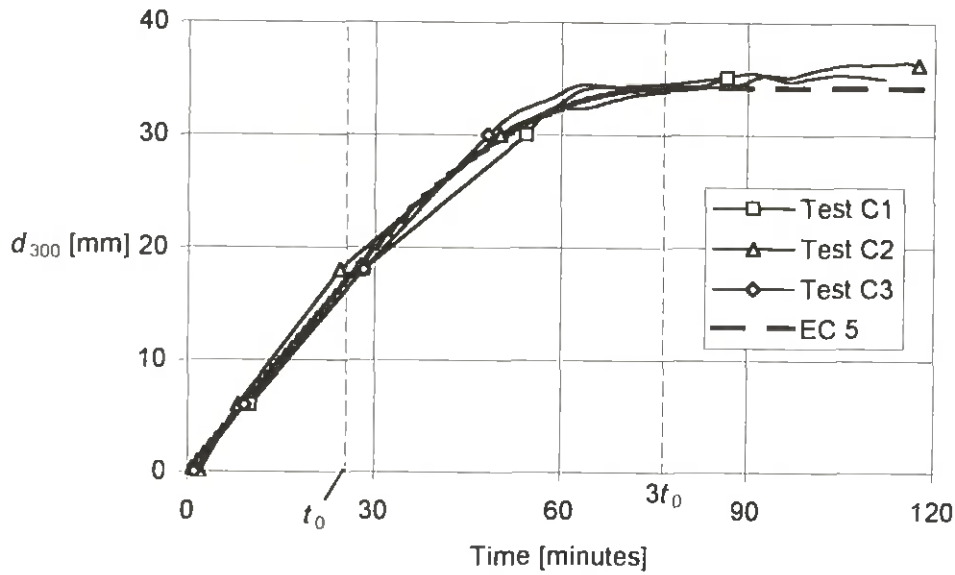


Figure 3.17: Charring depth versus time: Comparison of experimental curves with Eurocode 5

In tests C4-C6 the measured temperature in the furnace deviated considerably from the target curve 500/0,12, see Figure 2.20. Using the "fitted" parametric fire curves of Figure 2.20, we get the charring depth curves shown in Figure 3.18, where the parametric fire curve 300/0,06 corresponds to test C4 and 380/0,08 to test C6. We can see that, taking into account the deviations of the fitted curves from the measured ones, the expressions of Eurocode 5 agree fairly well with the tests results.

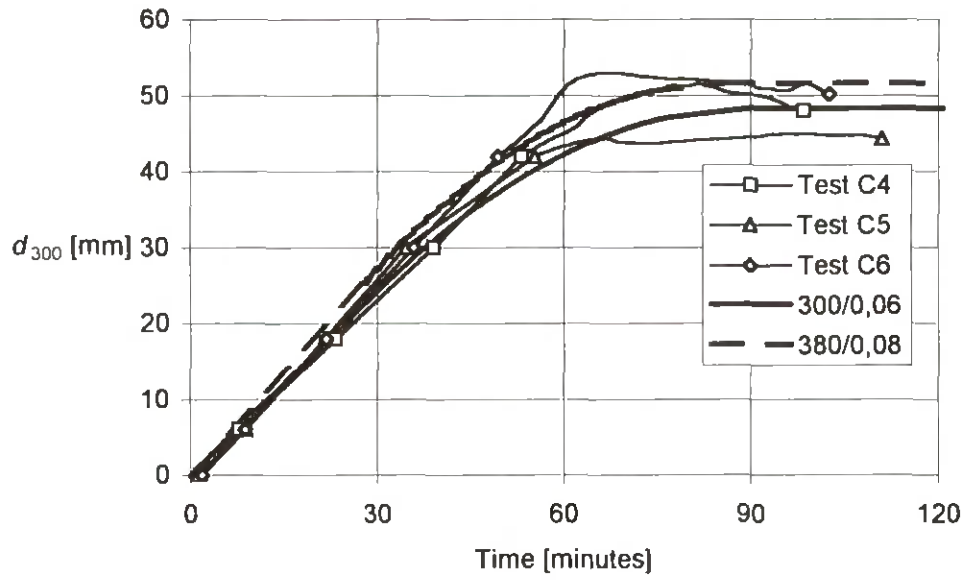


Figure 3.18: Charring depth versus time: Comparison of experimental curves with Eurocode 5

4 Conclusions

4.1 Tests

In this investigation, tests were performed where timber members with thermal conditions of a semi-infinite slab were exposed to standard and parametric fires.

When the members were unprotected right from the beginning, for standard fire exposure, the relationship between time and charring depth was slightly non-linear, however, for design purposes, it can be considered as linear. The mean charring rate, i.e. the secant value, varies linearly between 0,7 mm/minute after 20 minutes and 0,6 mm/minute after 90 minutes. The value given in the Fire Part of Eurocode 5¹ is 0,64 mm/minute and valid after 60 minutes. For shorter times, e.g. 30 to 40 minutes, a charring rate of 0,67 mm/minute is more appropriate.

For initially protected members, during the post-protection phase, the relationship between time and charring depth is pronounced non-linear with charring rates generally greater than the charring rate of initially unprotected members. For use in a design model, a linear or bi-linear model could replace the non-linear relationships. Using the charring rate of initially unprotected members also during the post-protection phase, as prescribed in ENV 1995-1-2¹ would give unsafe results.

The results of charring depths of tests with parametric fire exposure confirm the results obtained previously by Hadvig²¹ and Bolonius Olesen et al.²² and their adoption in the Fire Part of Eurocode 5¹.

4.2 Model

A general problem when using analytical models to calculate the heat transfer through structures is that, due to simplifications and deficiencies of the model, the thermal properties of the materials used as input parameters must be calibrated such that the results are fitted to those obtained by tests. Deviations from the real test conditions may be caused since the model does not take into account the

- mass transfer within the structure
- reaction energy released inside the wood due to pyrolysis
- degradation of material, e.g. the cracking of char coal which increases the heat transfer of the char layer.

Therefore, thermal properties found in different sources cannot generally be used in calculations. Thermal properties taken from different sources may give unduly conservative or unsafe results if they are used in the design without calibrating them to test results.

In the calculations, it was found that reaction heat during pyrolysis can be neglected.

Calculations using the thermal properties that were calibrated to test results with standard fire exposure overpredict the charring rate when the temperature rise is greater than at standard fire exposure, i.e. when the opening factor is greater than $0,04 \text{ m}^{1/2}$, whereas they underpredict the charring rate when the gas temperature is decreasing. This is probably also the case in the initial stage of a fire when the opening factor is smaller than $0,04 \text{ m}^{1/2}$.

It was also tried, however without success, to assume a heat source inside the member by using negative specific heat values in the pyrolysis zone. The negative effect of this manipulation was that the charring rate increased considerably above the test results.

For parametric fire curves, the thermal properties of wood and the char layer should be calibrated further in order to achieve a better agreement with the test results.

5 References

1. ENV 1995-1-2:1994, *Eurocode 5 - Design of timber structures, Part 1-2 Structural fire design*
2. König, J., 1998, Revision of ENV 1995-1-2: Charring and degradation of strength and stiffness. *CIB W18*, Meeting Thirty-One in Savonlinna, Paper 31-16-1, 1998
3. König, J., 1995, *Fire resistance of timber joists and load bearing wall frames*. Swedish Institute for Wood Technology Research, Report No. I 9412071
4. König J., Norén J., Bolonius Olesen F. & Toft Hansen F., 1997, *Timber frame assemblies exposed to standard and parametric fires - Part 1: Fire tests*. Swedish Institute for Wood Technology Research, Report No. I 9702015
5. König, J. & Walleij, L., *Timber frame assemblies exposed to standard and parametric fires - Part 2: Model for standard fire exposure*. Swedish Institute for Wood Technology Research. In preparation
6. Magnusson, S E & Thelandersson, S, *Temperature-time curves of complete process of fire development*. Acta Polytechnica Scandinavica, Stockholm 1970
7. Fire Safety Design, 1990, *User's Manual for TCD 3.0 with Tempcalc*. Lund
8. ASCE Committee on Fire Protection, Structural Division, 1992, *Structural fire protection*. New York
9. Roberts, A., F., 1971, The heat reaction during the pyrolysis of wood. *Combustion and Flame*, 17.
10. Mehaffey, J., R., Cuerrier, P., Carisse, G., 1994, A model for predicting heat transfer through gypsum board/wood stud walls exposed to fire. *Fire and materials*, Vol. 18.
11. Thomas, G. C. , 1997, *Fire resistance of light timber framed walls and floors*. University of Canterbury, Canterbury
12. Fredlund B., 1988, *A Model for Heat and Mass Transfer in Timber Structures during Fire*. Lund University, Lund
13. Fredlund B., 1993, Modelling of Heat and Mass Transfer in Timber Structures During Fire. *Fire Safety Journal*. Volume 20. Number 1.
14. Knudson, R. M., & Schniewind, A. P., 1975, Performance of structural wood members exposed to fire. *Forest Products Journal*, Vol. 25, No. 2
15. Janssens, M., Thermo-physical properties for wood pyrolysis models. *Pacific Timber Engineering Conference*, Gold Coast, Australia, 1994
16. Gammon, B. W., 1987, *Reliability analysis of wood-frame assemblies exposed to fire*. Ph.D. Dissertation. University of California, Berkeley, U.M.I. Dissertation Services, USA
17. Landolt-Börnstein, *Zahlenwerte und Funktionen aus Physik, Chemie, Astronomie, Geophysik, Technik*. Sechste Auflage, Band II, 4. Teil, Kalorische Zustandsgrößen, Springer Verlag 1961, Berlin, Göttingen, Heidelberg
18. Widell, T., 1948, *Thermal investigations into carbonization of wood*. Academy of Engineering Sciences, Report No. 199, Stockholm, Sweden
19. Tang, W. K., and Neill, W. K., *J. Polymer Sci.*, (c), 6, 65 (1964)
20. Fredlund, B., *Träets antändnings- och förbränningsmekanism*. Lund Institute of Technology, Department of Fire Safety Engineering, Internal report IR79-3, Lund
21. Hadvig, S., 1981, *Charring of wood in building fires*. Technical University of Denmark, Lyngby
22. Bolonius Olesen, F., & Hansen, T., 1992, *Full-scale tests on loaded glulam beams exposed to natural fires*. Aalborg University, Aalborg, Denmark

Detta digitala dokument
skapades med anslag från
**Stiftelsen Nils och Dorthi
Troëdssons forskningsfond**

Träte

INSTITUTET FÖR TRÄTEKNISK FORSKNING

Box 5609, 114 86 STOCKHOLM
Besöksadress: Drottning Kristinas väg 67
Telefon: 08-762 18 00
Telefax: 08-762 18 01

Åsensvägen 9, 553 31 JÖNKÖPING
Telefon: 036-30 65 50
Telefax: 036-30 65 60

Skeria 2, 931 77 SKELLEFTEÅ
Besöksadress: Laboratorgränd 2
Telefon: 0910-58 52 00
Telefax: 0910-58 52 65

Hemsida: www.tratek.se · E-post: tratek@tratek.se